NASA TECHNICAL NOTE

NASA TN D-8360

LOW-SPEED WIND-TUNNEL INVESTIGATION OF FLIGHT SPOILERS AS TRAILING-VORTEX-ALLEVIATION DEVICES ON A MEDIUM-RANGE WIDE-BODY TRI-JET AIRPLANE MODEL

Delwin R. Croom, Raymond D. Vogler, and Geoffrey M. Williams

Langley Research Center
Hampton, Va. 23665

NATIONAL AERONAUTICS AND SPACE ADMINISTRATION · WASHINGTON, D. C. · NOVEMBER 1976

1. Report No.	2. Government Accession No.	3. Recipient's Catalog No.
NASA TN D-8360		

4. Title and Subtitle	5. Report Date
LOW-SPEED WIND-TUNNEL INVESTIGATION OF FLIGHT SPOILERS AS TRAILING-VORTEX-ALLEVIATION DEVICES ON A MEDIUM-RANGE WIDE-BODY TRI-JET AIRPLANE MODEL	November 1976
	6. Performing Organization Code

7. Author(s)	8. Performing Organization Report No.
Delwin R. Croom, Raymond D. Vogler, and Geoffrey M. Williams	L-11103
	10. Work Unit No. 514-52-01-03
9. Performing Organization Name and Address NASA Langley Research Center Hampton, VA 23665	11. Contract or Grant No.
	13. Type of Report and Period Covered Technical Note
12. Sponsoring Agency Name and Address National Aeronautics and Space Administration Washington, DC 20546	14. Sponsoring Agency Code

15. Supplementary Notes

Delwin R. Croom and Raymond D. Vogler: Langley Research Center.
Geoffrey M. Williams: Lockheed-California Company, Burbank, California.

16. Abstract

An investigation was made in the Langley V/STOL tunnel to determine, by the trailing wing sensor technique, the effectiveness of various segments of the existing flight spoilers on a medium-range wide-body tri-jet transport airplane model when they were deflected as trailing-vortex-alleviation devices. The four combinations of flight-spoiler segments investigated were effective in reducing the induced rolling moment on the trailing wing model by as much as 15 to 60 percent at distances behind the transport model of from 3.9 to 19.6 transport wing spans, 19.6 spans being the downstream limit of distances used in this investigation. Essentially all of the reduction in induced rolling moment on the trailing wing model was realized at a spoiler deflection of about 45°.

17. Key Words (Suggested by Author(s))	18. Distribution Statement
Vortex alleviation Trailing-vortex hazard	Unclassified - Unlimited Subject Category 01

19. Security Classif. (of this report)	20. Security Classif. (of this page)	21. No. of Pages	22. Price*
Unclassified	Unclassified	46	$3.75

* For sale by the National Technical Information Service, Springfield, Virginia 22161

LOW-SPEED WIND-TUNNEL INVESTIGATION OF FLIGHT SPOILERS AS TRAILING-VORTEX-ALLEVIATION DEVICES ON A MEDIUM-RANGE WIDE-BODY TRI-JET AIRPLANE MODEL

Delwin R. Croom, Raymond D. Vogler,
and Geoffrey M. Williams*
Langley Research Center

SUMMARY

An investigation was made in the Langley V/STOL tunnel to determine, by the trailing wing sensor technique, the effectiveness of various segments of the existing flight spoilers on a medium-range wide-body tri-jet transport airplane model when they were deflected as trailing-vortex-alleviation devices. The four combinations of flight-spoiler segments investigated were effective in reducing the induced rolling moment on the trailing wing model by as much as 15 to 60 percent at distances behind the transport model of from 3.9 to 19.6 transport wing spans, 19.6 spans being the downstream limit of distances used in this investigation. Essentially all of the reduction in induced rolling moment on the trailing wing model was realized at a spoiler deflection of about 45°.

INTRODUCTION

The strong vortex wakes generated by large transport aircraft are a potential hazard to smaller aircraft. The National Aeronautics and Space Administration is involved in a program of model tests, flight tests, and theoretical studies to determine the feasibility of reducing this hazard by aerodynamic means.

Results of recent investigations have indicated that the trailing vortex behind an unswept-wing model (ref. 1) or a swept-wing transport model (ref. 2) can be attenuated by a forward-mounted spoiler. It was also determined by model tests (ref. 3) and verified in full-scale flight tests (ref. 4) that there are several combinations of the existing flight-spoiler segments on the jumbo-jet transport aircraft that are effective as trailing-vortex-alleviation devices. The approach used in references 1, 2, and 3 to evaluate the effectiveness of vortex-alleviation devices was to simulate an airplane flying in the trailing vortex of another larger airplane and to make direct measurments of rolling moments induced on the trailing model by the vortex generated by the forward model. The technique used in the full-scale flight test (ref. 4) was to penetrate the trailing vortex wake behind a Boeing 747 aircraft with a Cessna T-37 aircraft and to evaluate the roll response and roll attitude of the Cessna T-37 airplane as an index to the severity of the trailing-vortex encounter.

*Lockheed-California Company, Burbank, California.

The purpose of the present investigation is to determine the trailing-vortex-alleviation effectiveness of various segments of the existing flight spoiler of a medium-range wide-body tri-jet transport aircraft model. The direct-measurement technique described in references 1, 2, and 3 was used with the trailing wing model from 3.9 to 19.6 transport wing spans behind the transport aircraft model. (For the full-scale transport airplane, this would represent a range of downstream distance from 0.1 to 0.5 nautical mile.)

SYMBOLS

All data are referenced to the wind axes. The pitching-moment coefficients are referenced to the quarter-chord of the wing mean aerodynamic chord.

b wing span, m

C_D drag coefficient, $\frac{\text{Drag}}{qS_W}$

C_L lift coefficient, $\frac{\text{Lift}}{qS_W}$

$C_{l,TW}$ trailing wing rolling-moment coefficient, $\frac{\text{Trailing wing rolling moment}}{qS_{TW}b_{TW}}$

C_m pitching-moment coefficient, $\frac{\text{Pitching moment}}{qS_W\bar{c}_W}$

c wing chord, m

$\bar{c}$ wing mean aerodynamic chord, m

i_t horizontal-tail incidence, referred to fuselage reference line (positive direction trailing edge down), deg

l longitudinal distance in tunnel diffuser, m

q dynamic pressure, Pa

S wing area, m^2

X',Y',Z' system of axes originating at left wing tip of transport aircraft model (see fig. 1)

x',y',z' longitudinal, lateral, and vertical dimensions measured from trailing edge of left wing tip of transport aircraft model, m

$\Delta y',\Delta z'$ incremental dimensions along Y'- and Z'-axes, m

α angle of attack of fuselage reference line, deg (wing root incidence is 3^o relative to fuselage reference line)

δ deflection, deg

ϕ local streamline angle in tunnel diffuser relative to tunnel center line, deg

Subscripts:

flap transport aircraft model flap

max maximum

slat transport aircraft model slat

spoiler transport aircraft model spoiler

TW trailing wing model

vane transport aircraft model vane

W transport aircraft model

MODEL AND APPARATUS

A three-view sketch and principal geometric characteristics of the 0.05-scale model of a medium-range wide-body tri-jet transport aircraft (Lockheed L-1011) are shown in figure 1. Sketches of the landing and approach flap configurations are shown in figures 2 and 3, respectively. Figure 4 is a photograph of the transport aircraft model sting mounted in the Langley V/STOL tunnel. Figure 5 is a sketch showing the location of the flight spoilers on the transport aircraft model. Photographs of the four combinations of flight-spoiler segments investigated are presented in figure 6.

The test section of the Langley V/STOL tunnel has a height of 4.42 m, a width of 6.63 m, and a length of 14.24 m. The transport aircraft model was sting supported on a six-component strain-gage balance system which measured the forces and moments. The angle of attack was determined from an accelerometer mounted in the fuselage.

A photograph and dimensions of the unswept trailing wing model installed on a traverse mechanism are presented in figure 7. The trailing model has a span and aspect ratio typical of small-size transport aircraft. The trailing model was mounted on a single-component strain-gage roll balance, which was attached to the traverse mechanism capable of moving both laterally and vertically. (See fig. 7.) The lateral and vertical positions of the trailing model were measured by outputs from digital encoders. This entire traverse mechanism could be mounted to the tunnel floor at various tunnel longitudinal positions downstream of the transport aircraft model.

TESTS AND CORRECTIONS

Transport Aircraft Model

All tests were made at a free-stream dynamic pressure (in the tunnel test section) of 430.9 Pa, which corresponds to a velocity of 27.4 m/sec. The Reynolds number for these tests was approximately 6.8×10^5 based on the wing mean aerodynamic chord. No transition grit was applied to the transport aircraft model. The basic longitudinal aerodynamic characteristics were obtained through an angle-of-attack range of approximately -4° to 22°. All tests were made with leading-edge devices and landing gear extended.

Blockage corrections were applied to the data by the method of reference 5. Jet-boundary corrections to the angle of attack and the drag were applied in accordance with reference 6.

Trailing Wing Model

The trailing wing model and its associated roll-balance system were used as a sensor to measure the induced rolling moment caused by the vortex flow downstream of the transport aircraft model. No transition grit was applied to the trailing model. The trailing model was positioned at a given distance downstream of the transport aircraft model on the traverse mechanism which was positioned laterally and vertically so that the trailing vortex was near the center of the mechanism. The trailing vortex was probed with the trailing model. A large number of trailing wing rolling-moment data points (usually from 50 to 100) were obtained from the lateral traverses at several vertical locations to ensure good definition of the vortex wake. In addition, certain test conditions were repeated at selected intervals during the test period and the data were found to be repeatable.

Trailing wing rolling-moment measurements were made at downstream scale distances from about 3.9 to 19.6 transport wing spans behind the transport aircraft model. All trailing wing rolling-moment data at distances downstream greater than about 3.9 spans were obtained with the trailing model positioned in the diffuser section of the V/STOL tunnel. These data were reduced to coefficient form based on the dynamic pressure at the trailing wing location. For these tests, the dynamic pressures at the 3.92, 9.81, and 19.61 span locations were 430.9, 287.0, and 88.38 Pa, respectively. The trailing wing location relative to the wing tip of the transport aircraft model has been corrected to account for the progressively larger tunnel cross-sectional area in the diffuser section. The corrections to the trailing wing location in the diffuser were made by assuming that the local streamline angles in the tunnel diffuser section are equal to the ratio of the distance from the tunnel center line to the local tunnel half-width or tunnel half-height multiplied by the diffuser half-angle. Corrections to the trailing model locations are as follows: $\Delta y'$ correction or $\Delta z'$ correction $= \iota \tan \phi$ where $\Delta y'$ correction and $\Delta z'$ correction are, respectively, the corrections to the measured lateral and vertical locations of the trailing model relative to the tip of the transport aircraft model, ι is the longitudinal distance in the tunnel diffuser, and ϕ

is the local streamline angle in the tunnel diffuser relative to the tunnel center line.

RESULTS AND DISCUSSION

Transport Aircraft Model

The longitudinal aerodynamic characteristics of the transport aircraft model in the landing flap configuration with spoilers retracted (see fig. 2) are presented in figure 8. These data were obtained over a range of horizontal-tail incidence sufficient to trim the model through the range of lift coefficient. These data indicate that the transport aircraft model was statically stable up to the stall. The static margin, dC_m/dC_L, for the model was about -0.24.

The longitudinal aerodynamic characteristics of the transport aircraft model with flight-spoiler segments 1 and 2, 2 and 3, 3 and 4, and 1 and 4 deflected symmetrically through a spoiler deflection range of from 0° to 60° are presented in figures 9, 10, 11, and 12, respectively, for the landing flap configuration and in figures 13, 14, 15, and 16, respectively, for the approach flap configuration. These data were obtained with $i_t = 0^\circ$. For both of these configurations, there was essentially a linear increase in drag with spoiler deflection. For the landing flap configuration, about 50 percent of the lift loss at a given angle of attack occurred at a spoiler deflection of about 15°. For the approach flap configuration, about 50 percent of the lift loss at a given angle of attack occurred at a spoiler deflection of about 30°. The variation of pitching-moment coefficient with angle of attack was generally more linear when the spoilers were deflected than when they were retracted.

The longitudinal aerodynamic characteristics of the transport aircraft model with the four combinations of flight spoilers on each wing deflected symmetrically 45° are presented in figures 17 and 18 for the landing flap configuration and the approach flap configuration, respectively. These data indicate that for the landing flap configuration (fig. 17) a nominal lift coefficient of 1.2 can be maintained with an increase in angle of attack of no more than 3° for any of the spoiler configurations tested. It can also be seen in figure 17 that the maximum increase in drag coefficient at $C_L = 1.2$, for any of the spoiler configurations, was about 0.05 and that the maximum lift coefficient was reduced by about 0.14. For the approach flap configuration (fig. 18) a nominal lift coefficient of 1.2 can be maintained with no more than a 2° increase in angle of attack for any of the spoiler combinations investigated. The drag penalty due to spoilers was no more than 0.04 and the reduction in maximum lift coefficient was no more than 0.08 for any of the spoiler configurations investigated. It can also be seen in figures 17 and 18 that, for both flap configurations, the variation of pitching-moment coefficient with angle of attack was generally more linear when the spoilers were deflected than when they were retracted.

Trailing Wing Model

The maximum rolling-moment coefficient measured by the trailing model and the position of this model relative to the left wing tip of the transport aircraft model are presented as a function of flight-spoiler deflection for the various combinations of flight spoilers investigated in figures 19 to 22. The data presented in figure 19 are for the approach flap configuration with the trailing model positioned 9.8 transport wing spans behind the transport aircraft model. The data presented in figures 20, 21, and 22 are for the landing flap configuration with the trailing model positioned 3.9, 9.8, and 19.6 wing spans, respectively, behind the transport aircraft model. It can be seen in figures 19 to 22 that for any of the flight-spoiler-segment combinations tested, essentially all of the reduction in induced rolling moment was realized with about 45° of spoiler deflection.

The maximum rolling-moment coefficient measured by the trailing wing model and the position of this model relative to the left wing tip of the transport aircraft model are presented in figures 23 and 24 for the approach flap configuration and the landing flap configuration, respectively. These measurements were made at several downstream distances from the transport aircraft model with the flight spoilers retracted and with various flight-spoiler segments deflected 45°. It can be seen in figures 23 and 24 that when the flight spoilers were retracted the induced rolling moment on the trailing model at downstream distances greater than 4 transport spans was somewhat larger for the approach flap configuration than for the landing flap configuration. It can also be seen that all combinations of flight spoilers investigated were effective in reducing the induced rolling moment on the trailing model for both the approach and the landing flap configurations (a reduction of at least 15 percent). The largest reduction in induced rolling moment for both flap configurations was realized with spoiler segments 3 and 4 (reduction of the order of 35 to 60 percent). Of particular interest is the ability of spoiler segments 3 and 4 to effect a large reduction in $(C_{l,TW})_{max}$ (35 to 45 percent) in a relative near distance (about 4 transport wing spans) downstream of the transport aircraft model. The attenuated values of $(C_{l,TW})_{max}$ obtained with flight-spoiler segments 3 and 4 in the present wind-tunnel investigation are comparable with those obtained in the wind-tunnel test of the jumbo-jet transport aircraft reported in reference 3. Flight spoilers were shown to be effective in attenuating the trailing vortex in full-scale flight tests of the jumbo-jet transport aircraft (ref. 4); therefore, it appears that the flight spoilers on the present medium-range tri-jet transport aircraft would also be effective in attenuating the trailing vortex behind this aircraft.

SUMMARY OF RESULTS

Results have been presented of an investigation in the Langley V/STOL tunnel to determine, by the trailing wing sensor technique, the trailing-vortex-alleviation effectiveness of various segments of the flight spoilers on a medium-range tri-jet transport aircraft model when the segments are deflected as trailing-vortex-alleviation devices.

Four combinations of flight-spoiler segments were investigated and all were effective in reducing the induced rolling moment on the trailing wing model throughout the range of downstream distance used in this investigation. The largest reduction was realized with the two innermost spoiler segments investigated (a reduction of from 35 to 60 percent).

Results from tests of the four flight-spoiler configurations made over a deflection range from 0° to 60° indicate that essentially all of the reduction in induced rolling moment on the trailing model was realized at a spoiler deflection of about 45°.

Langley Research Center
National Aeronautics and Space Administration
Hampton, VA 23665
October 12, 1976

REFERENCES

1. Croom, Delwin R.: Low-Speed Wind-Tunnel Investigation of Forward-Located Spoilers and Trailing Splines as Trailing-Vortex Hazard-Alleviation Devices on an Aspect-Ratio-8 Wing Model. NASA TM X-3166, 1975.

2. Croom, Delwin R.; and Dunham, R. Earl, Jr.: Low-Speed Wind-Tunnel Investigation of Span Load Alteration, Forward-Located Spoilers, and Splines as Trailing-Vortex-Hazard Alleviation Devices on a Transport Aircraft Model. NASA TN D-8133, 1975.

3. Croom, Delwin R.: Low-Speed Wind-Tunnel Investigation of Various Segments of Flight Spoilers as Trailing-Vortex-Alleviation Devices on a Transport Aircraft Model. NASA TN D-8162, 1976.

4. Barber, Marvin R.; Hastings, Earl C., Jr.; Champine, Robert A.; and Tymczyszyn, Joseph J.: Vortex Attenuation Flight Experiments. Wake Vortex Minimization. NASA SP-409, 1976.

5. Herriot, John G.: Blockage Corrections for Three-Dimensional-Flow Closed-Throat Wind Tunnels, With Consideration of the Effect of Compressibility. NACA Rep. 995, 1950. (Supersedes NACA RM A7B28.)

6. Gillis, Clarence L.; Polhamus, Edward C.; and Gray, Joseph L., Jr.: Charts for Determining Jet-Boundary Corrections for Complete Models in 7- by 10-Foot Closed Rectangular Wind Tunnels. NACA WR L-123, 1945. (Formerly NACA ARR L5G31.)

WING	
Span, m	2.362
Mean aerodynamic chord, m	0.373
Sweepback at quarter-chord, deg	35
Area, m^2	0.8025
Aspect ratio	6.95
Taper ratio	0.30
FUSELAGE	
Length, m	2.582
HORIZONTAL TAIL	
Span, m	1.089
Area, m^2	0.2975
Aspect ratio	4.0

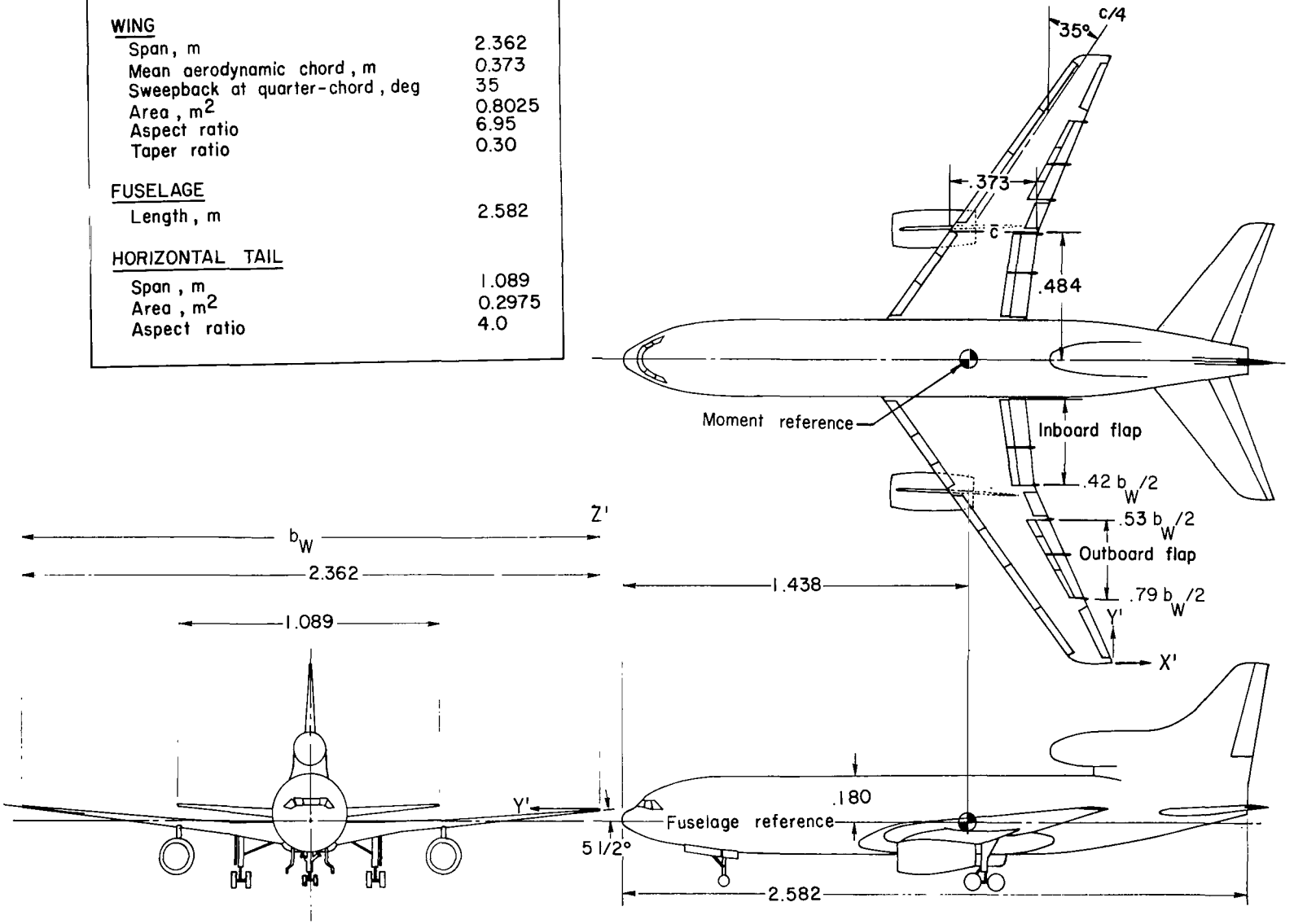

Figure 1.- Three-view sketch of transport aircraft model with flaps retracted. Linear dimensions are in meters.

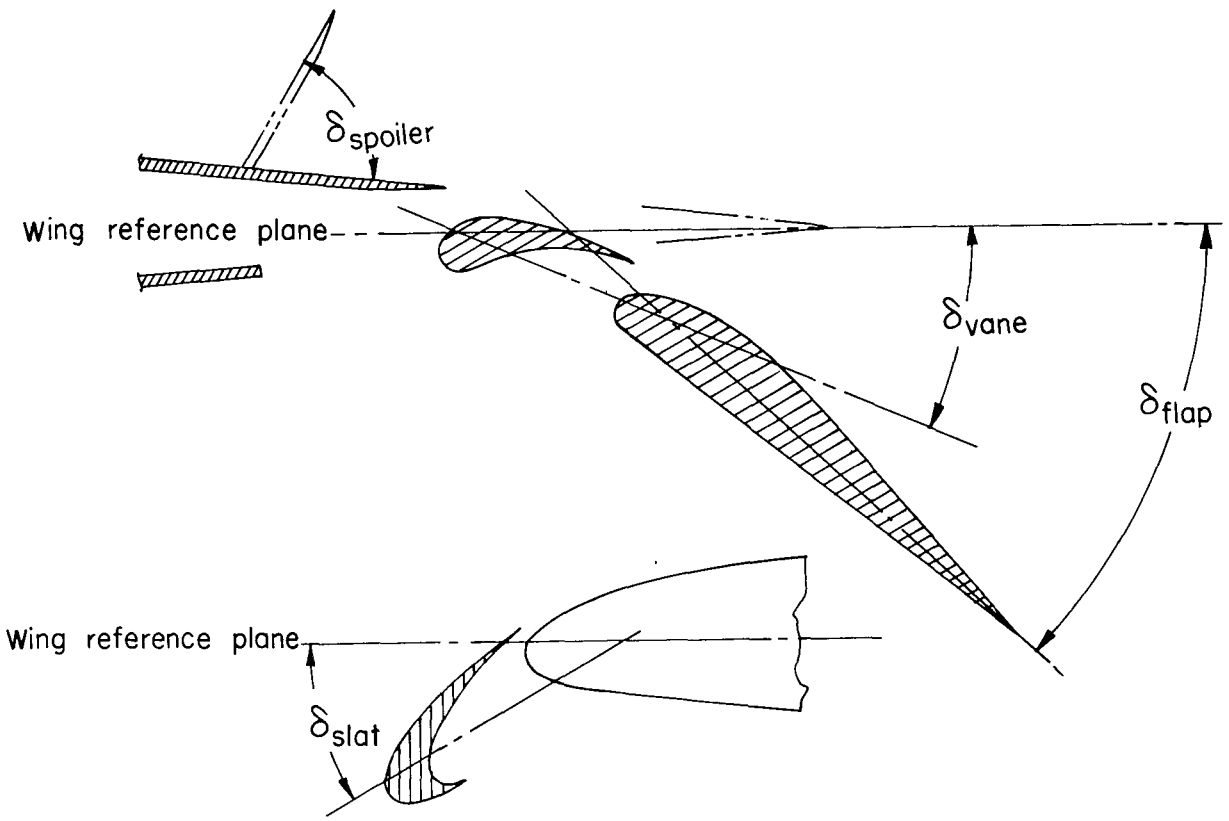

	Inboard	Outboard
δflap	45°	41°
δvane	25°	23°
δslat	28°	30°

Figure 2.- Sketch of spoiler and high-lift devices for landing configuration.

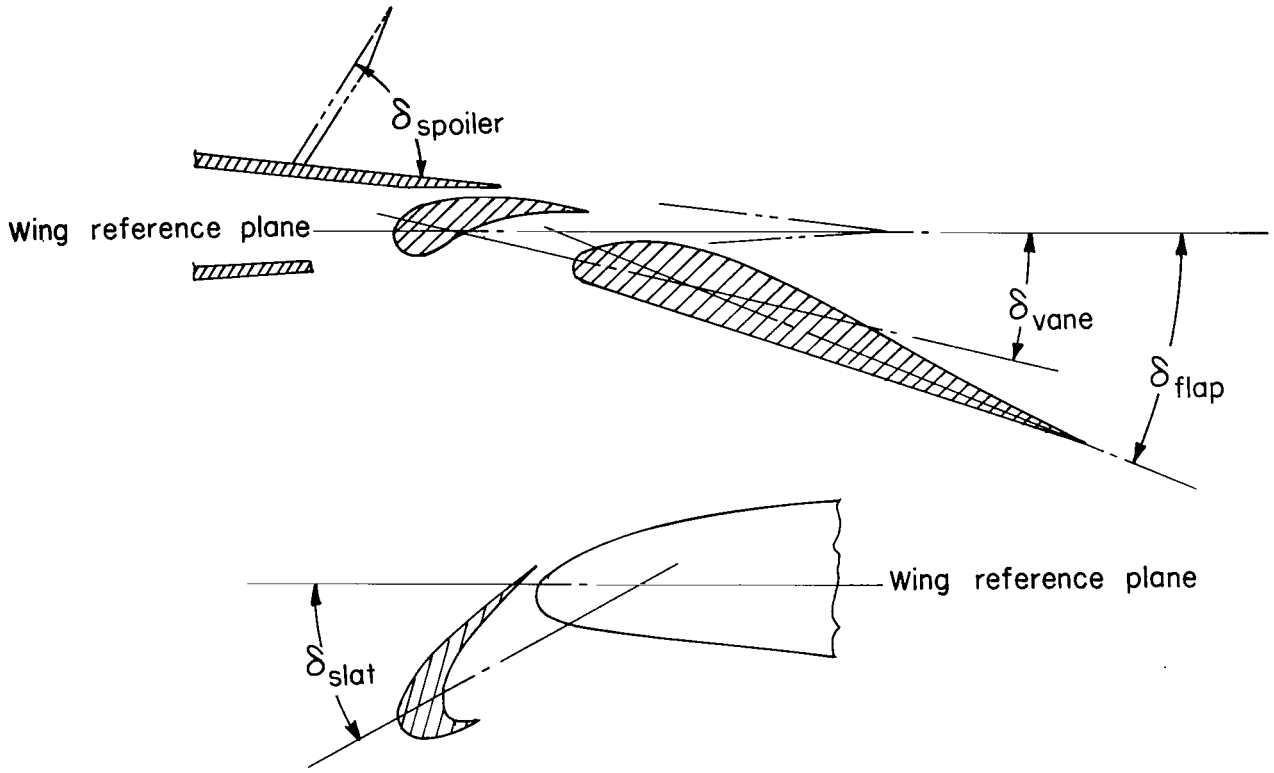

	Inboard	Outboard
δ_{flap}	26°	23°
δ_{vane}	16°	14°
δ_{slat}	28°	30°

Figure 3.- Sketch of spoiler and high-lift devices for approach configuration.

L-76-3209

Figure 4.- Photograph of test setup in Langley V/STOL tunnel.

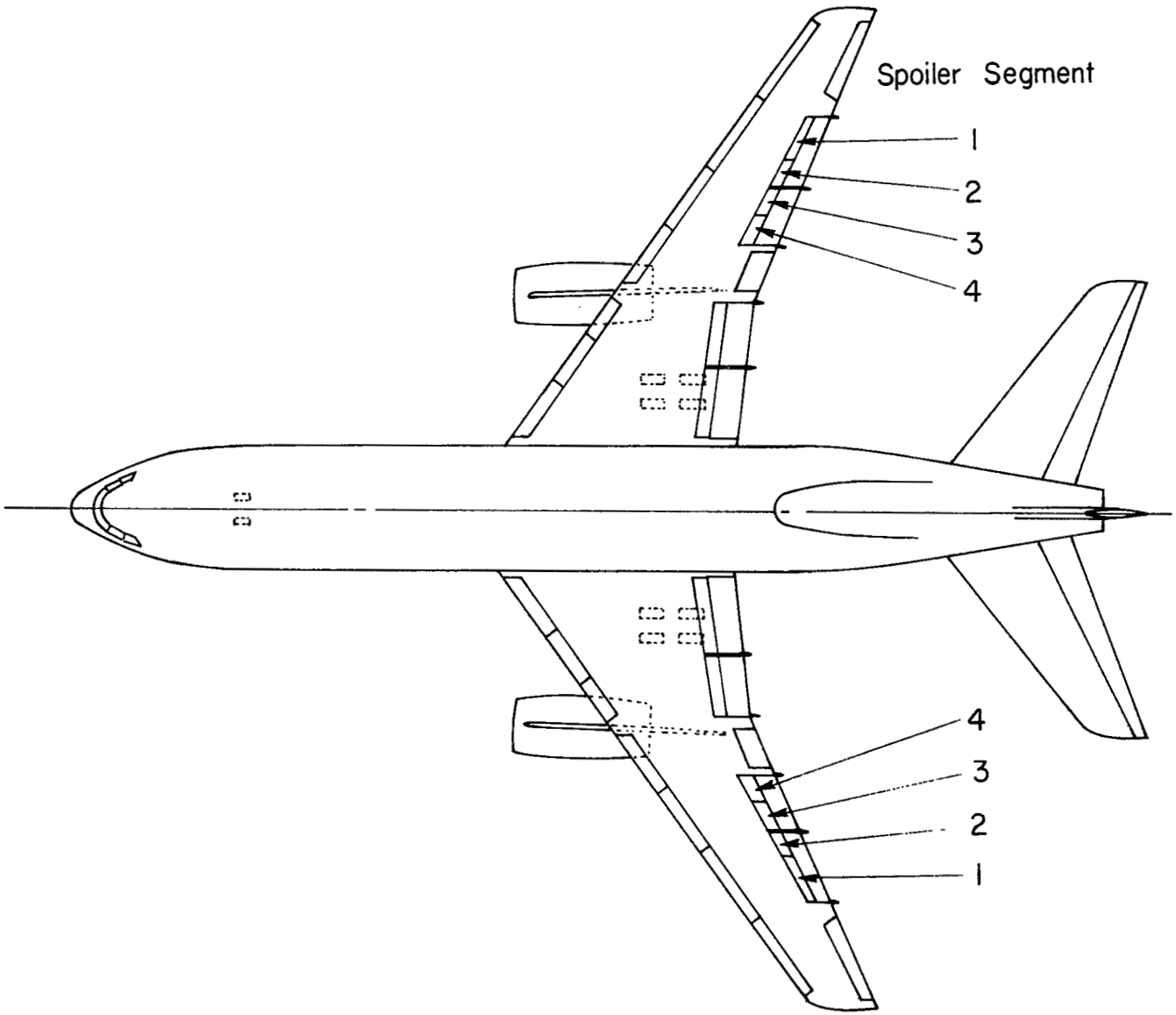

Figure 5.- Sketch of flight spoilers on transport aircraft model.

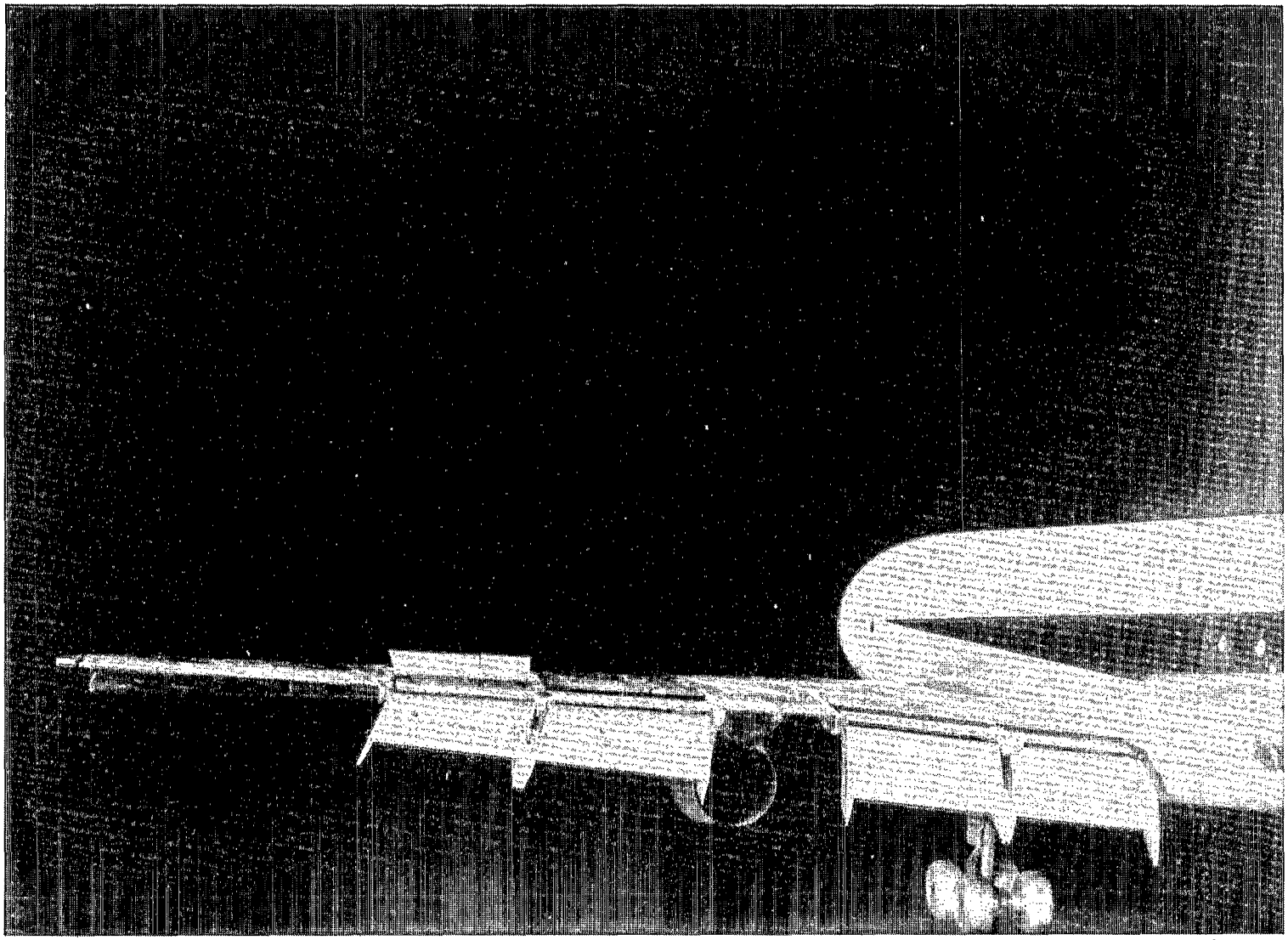

L-76-3211

(a) Spoiler segments 1 and 2 deflected 45°.

Figure 6.- Photographs of flight spoilers on transport aircraft model.

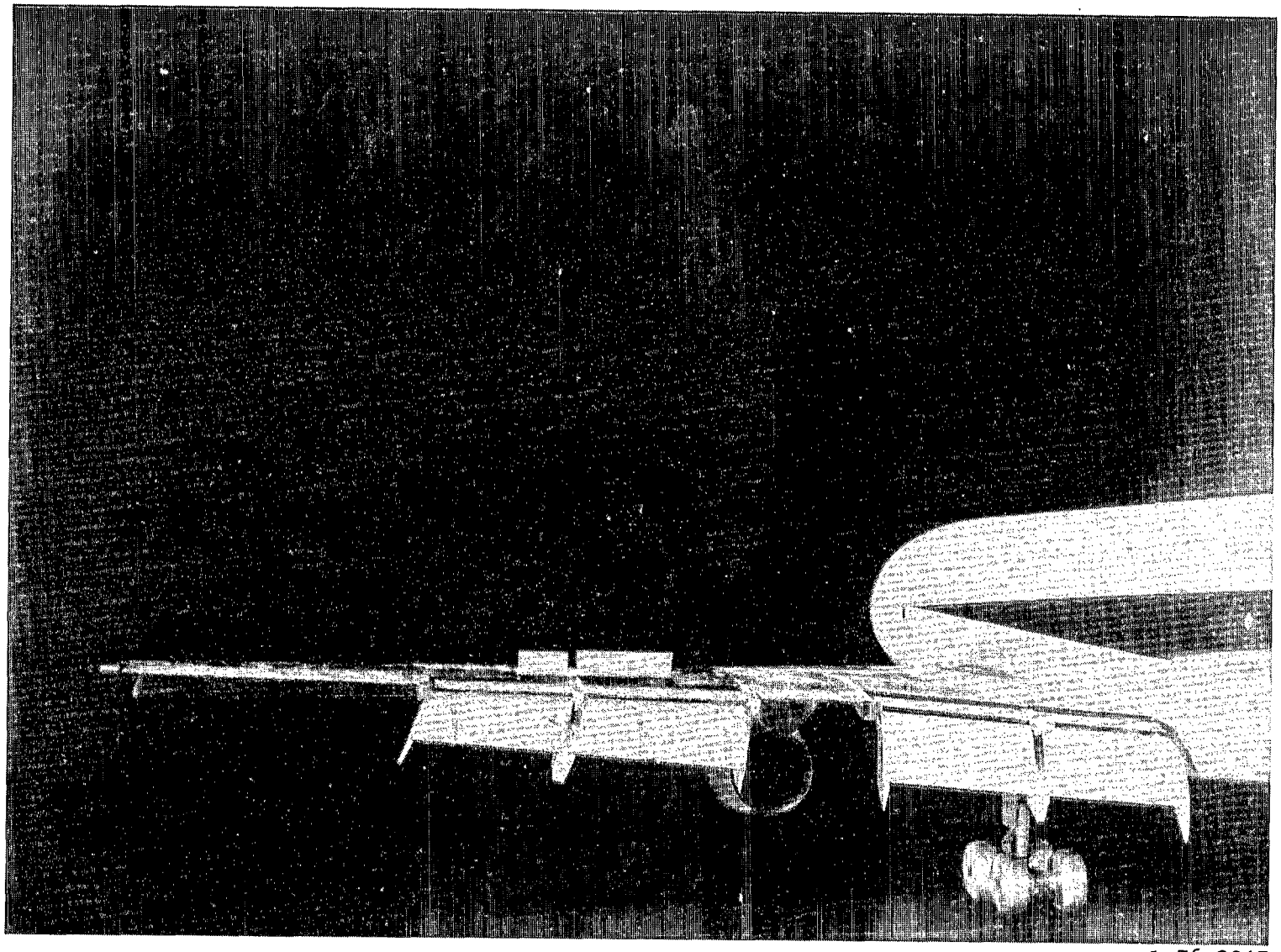

L-76-3215

(b) Spoiler segments 2 and 3 deflected 45°.

Figure 6.- Continued.

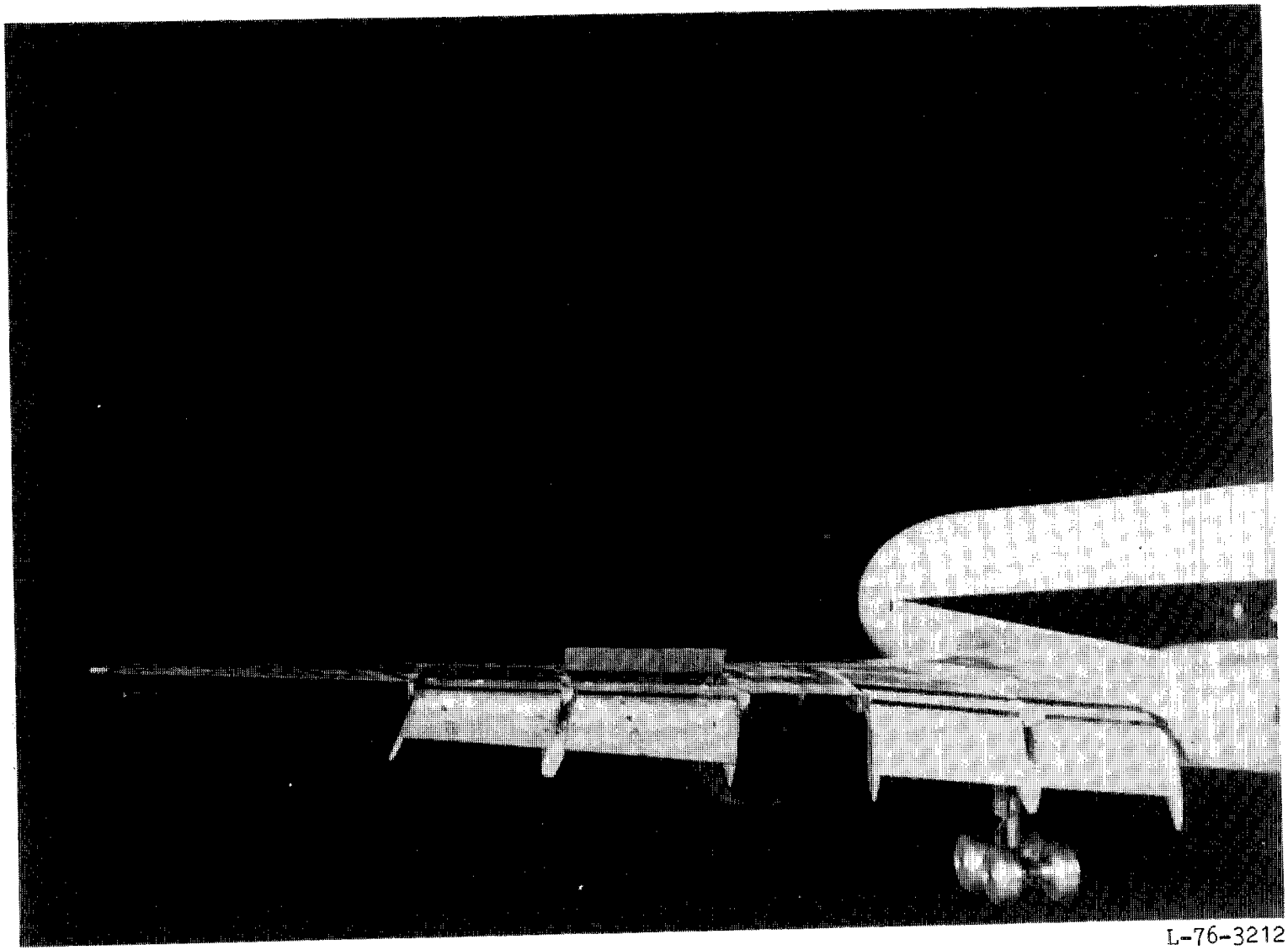

L-76-3212

(c) Spoiler segments 3 and 4 deflected 45°.

Figure 6.- Continued.

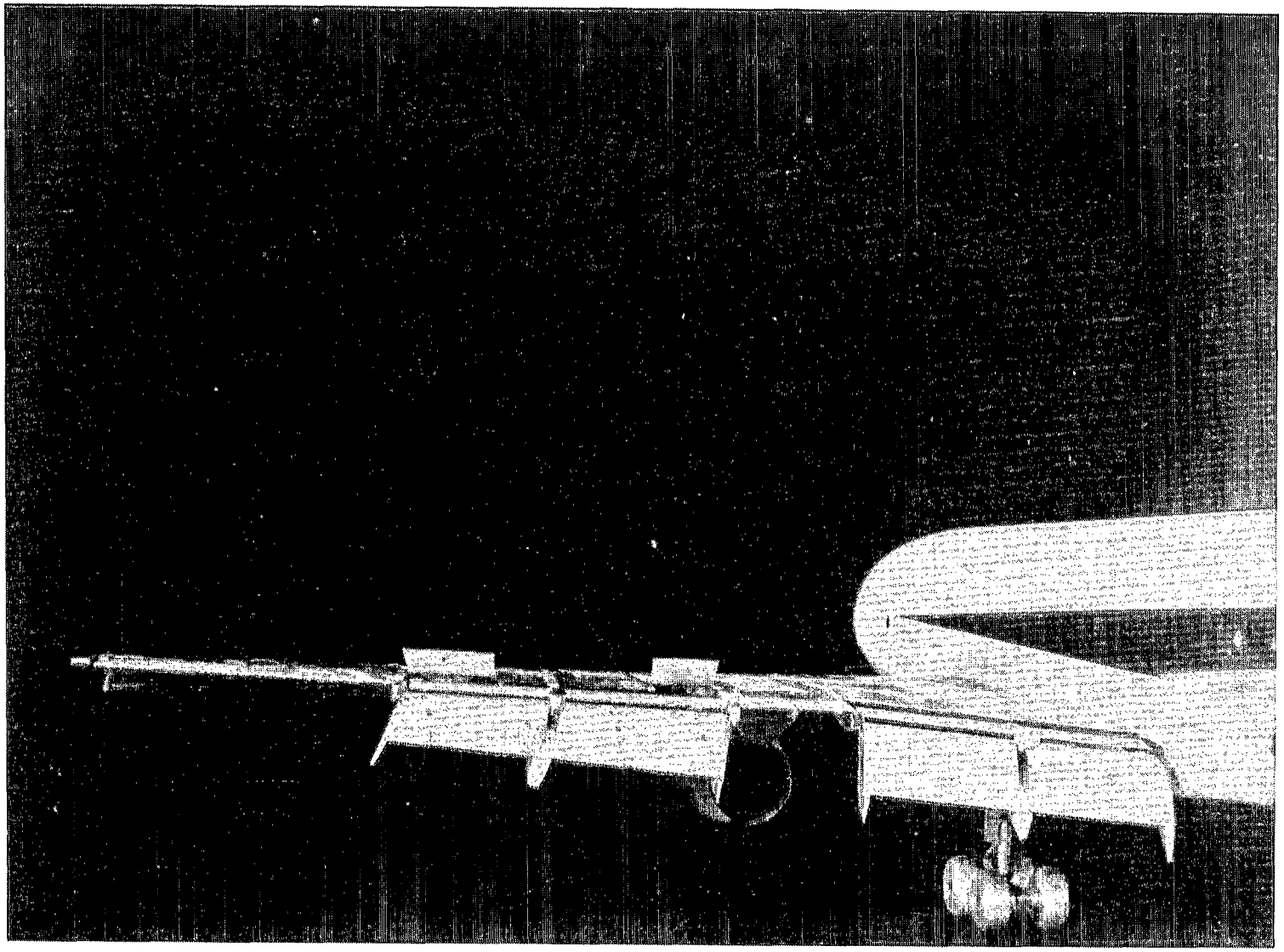

L-76-3213

(d) Spoiler segments 1 and 4 deflected 45°.

Figure 6.- Concluded.

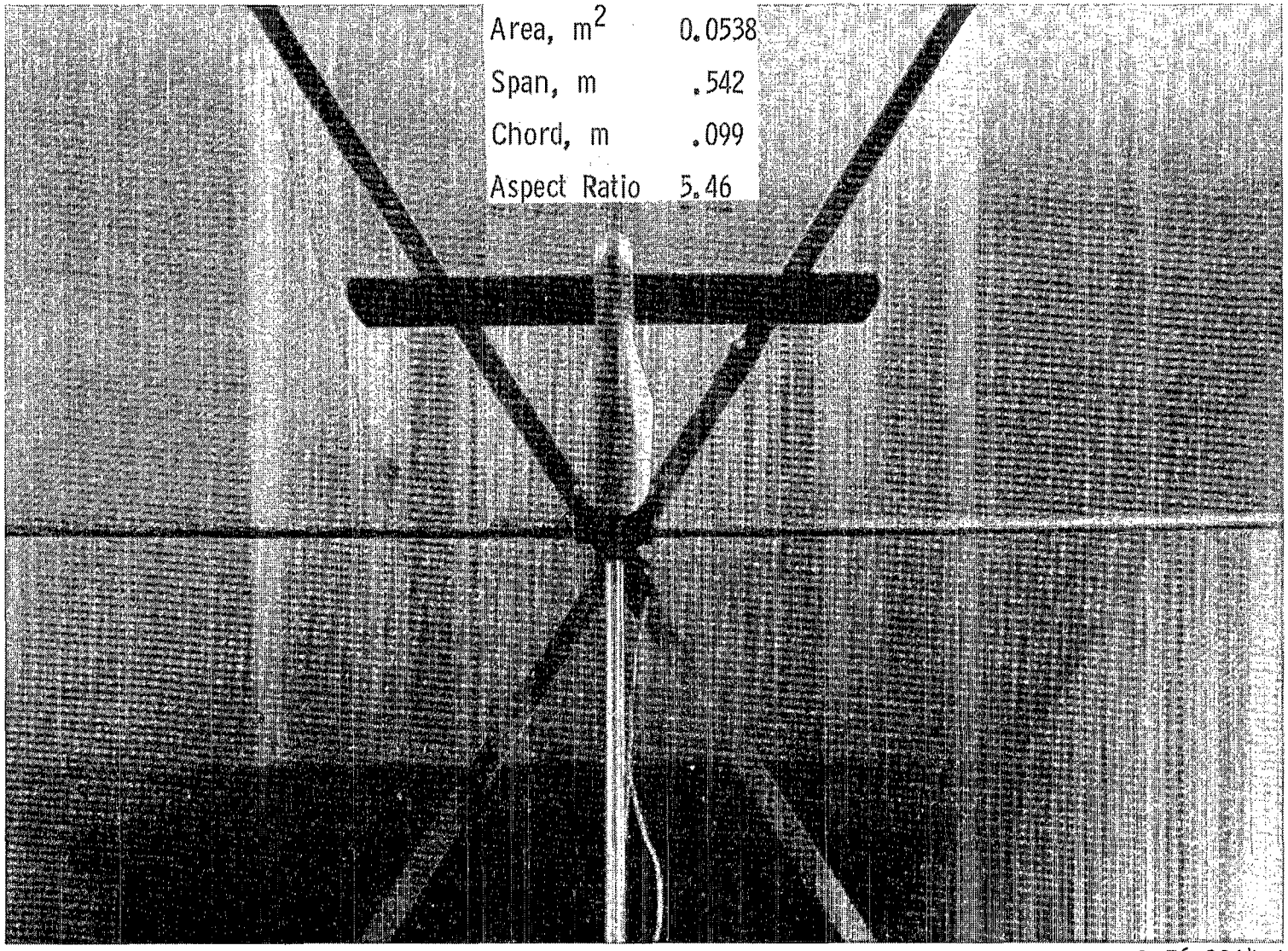

L-76-3214.1

Figure 7.- Photograph and dimensions of unswept trailing wing model on traverse mechanism. Model has NACA 0012 airfoil section.

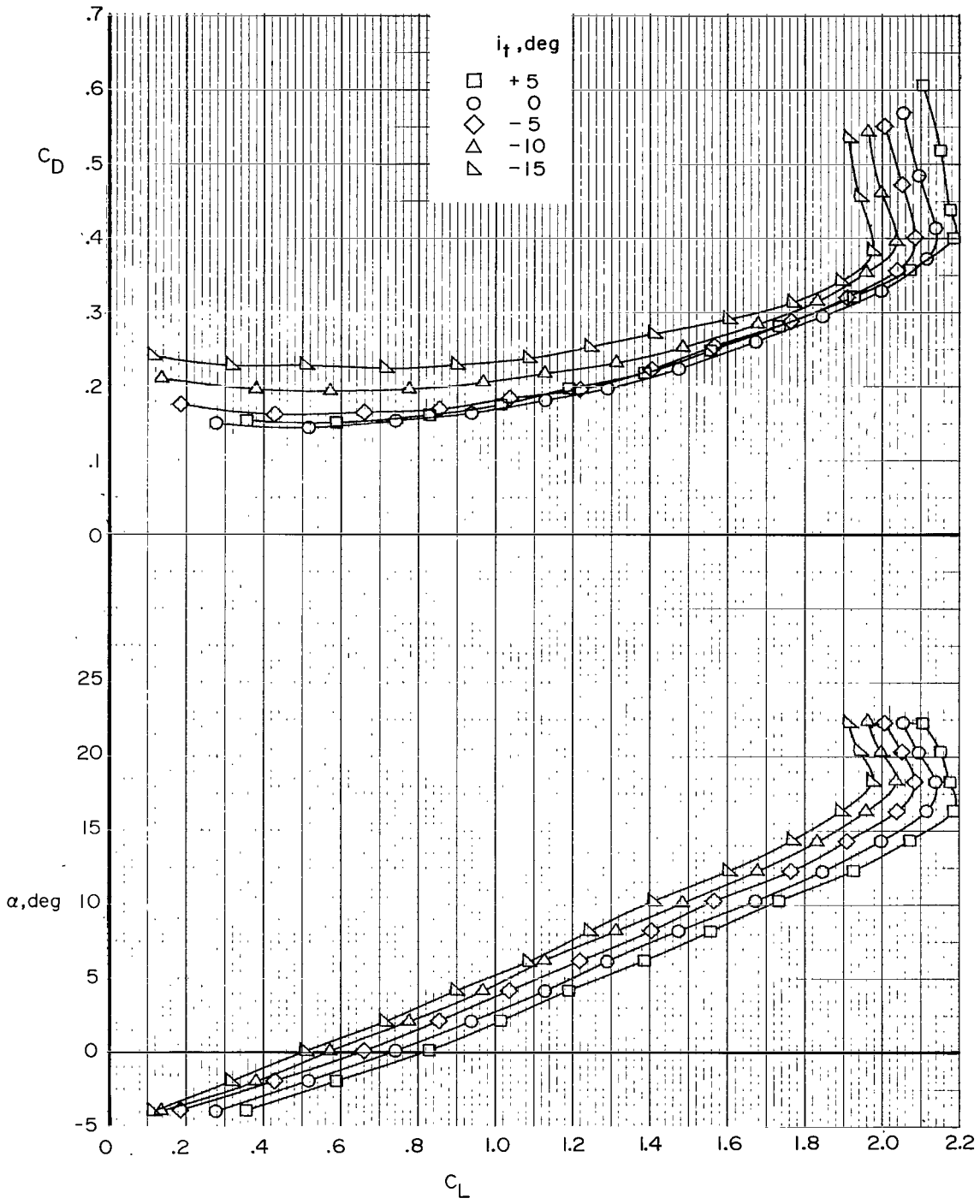

(a) Lift and drag coefficients.

Figure 8.- Effect of horizontal-tail incidence on longitudinal aerodynamic characteristics of transport aircraft model. Landing flap configuration.

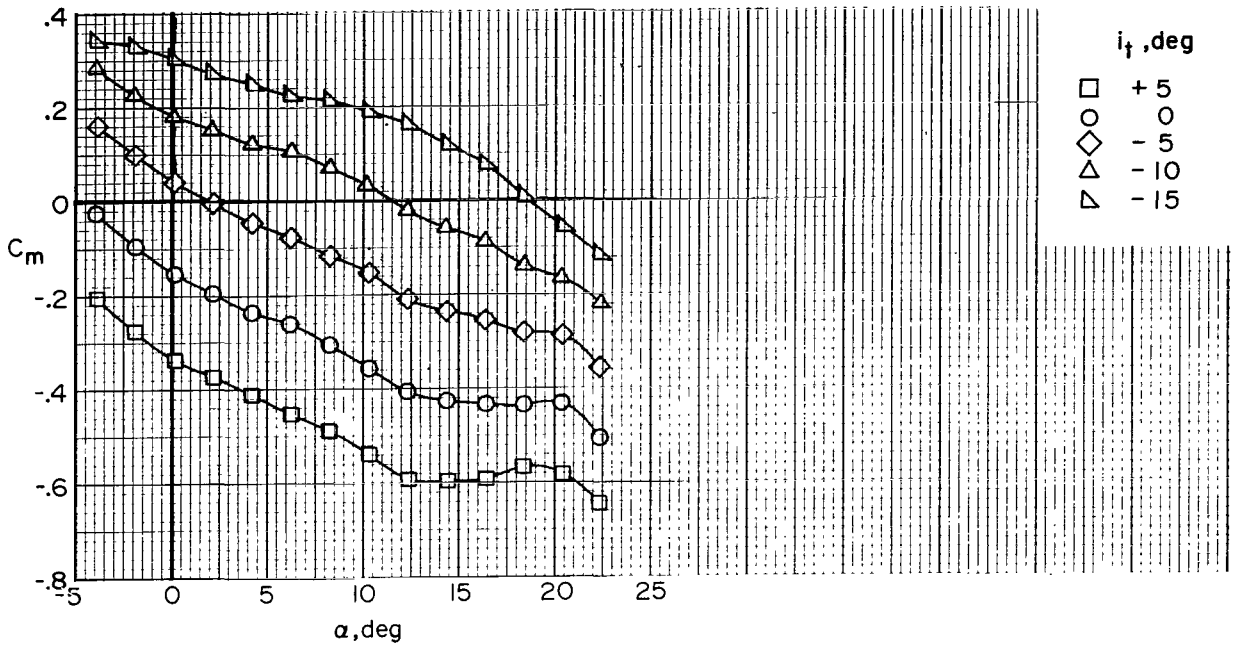

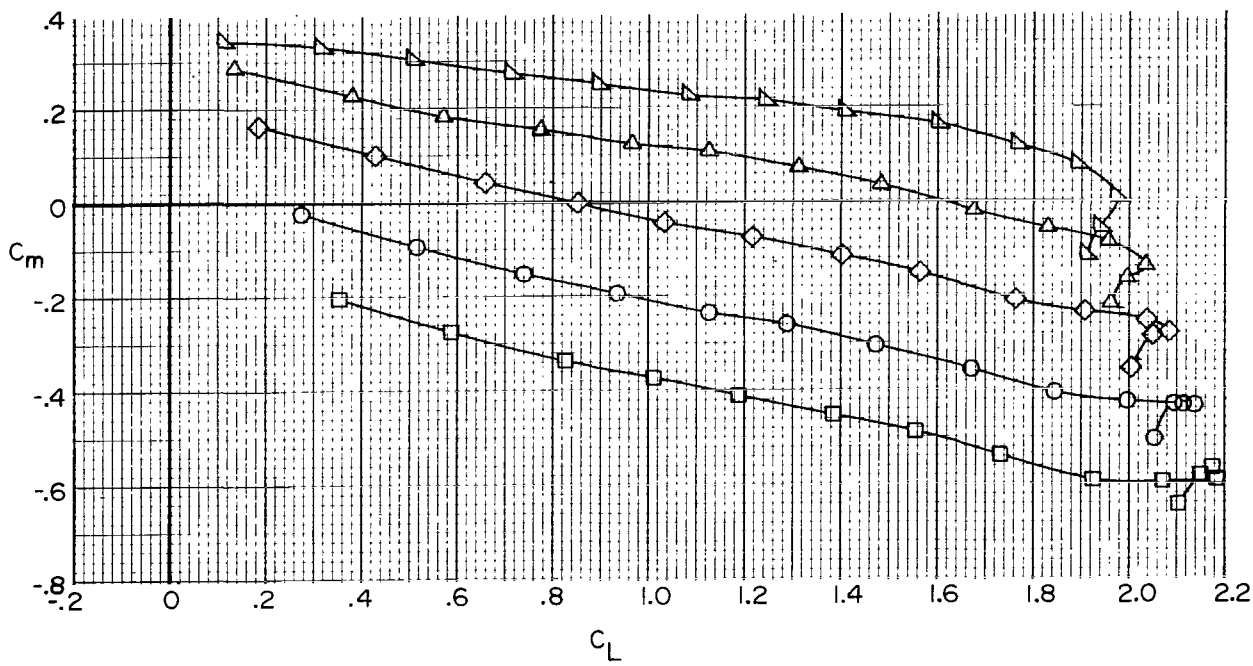

(b) Pitching-moment coefficient.

Figure 8.- Concluded.

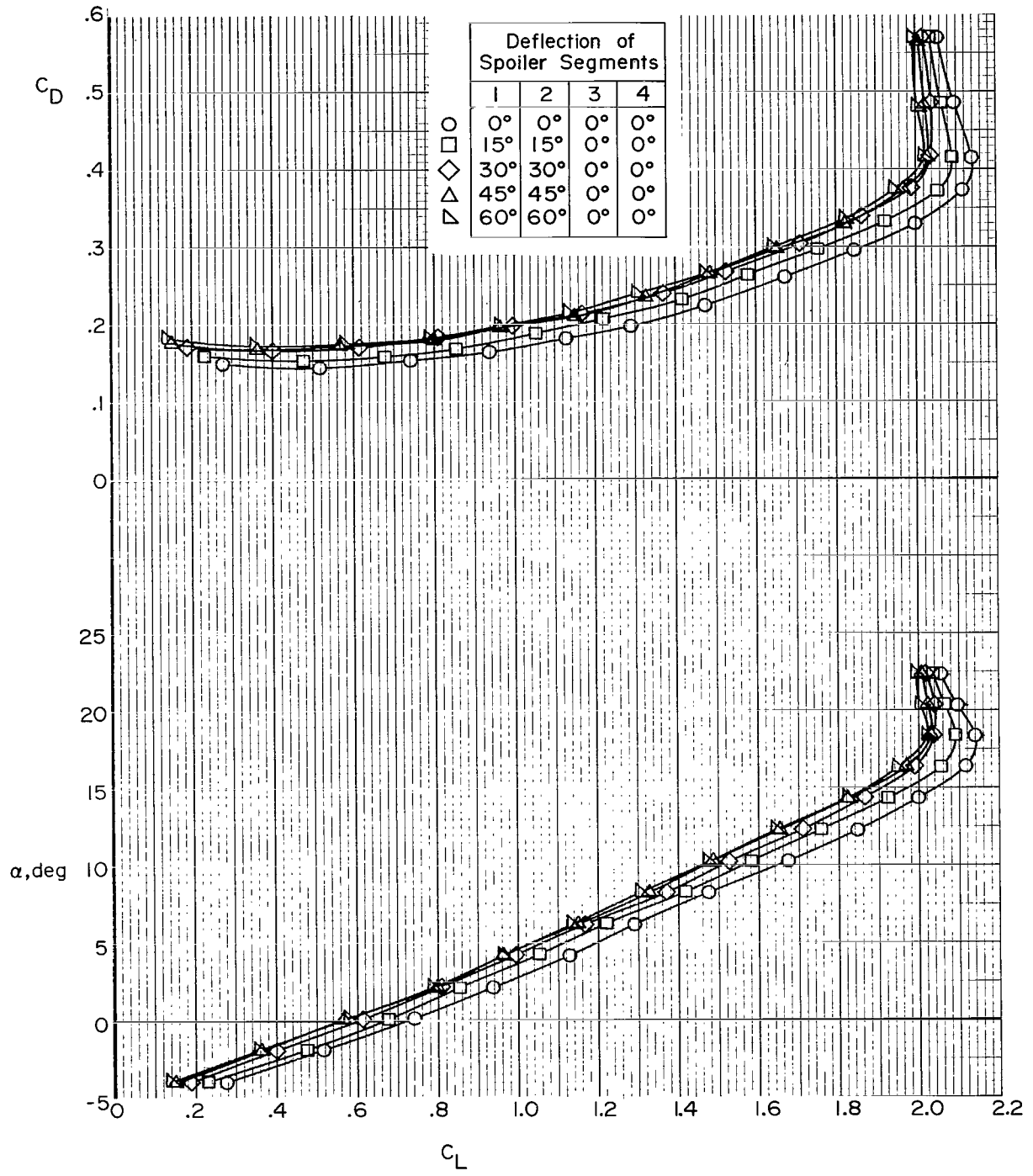

(a) Lift and drag coefficients.

Figure 9.- Effect of deflection angle of flight-spoiler segments 1 and 2 on longitudinal aerodynamic characteristics of transport aircraft model. $i_t = 0^\circ$; landing flap configuration.

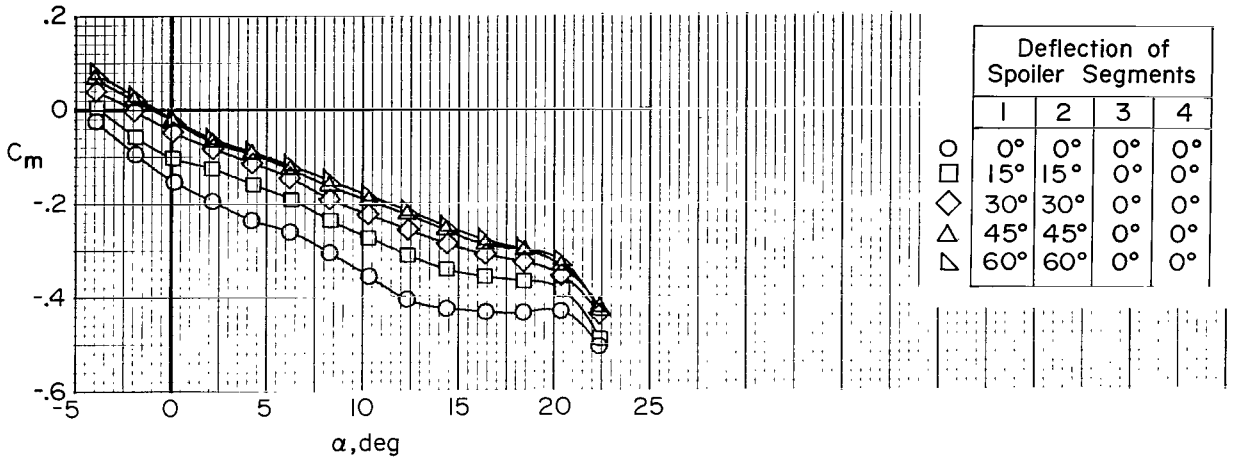

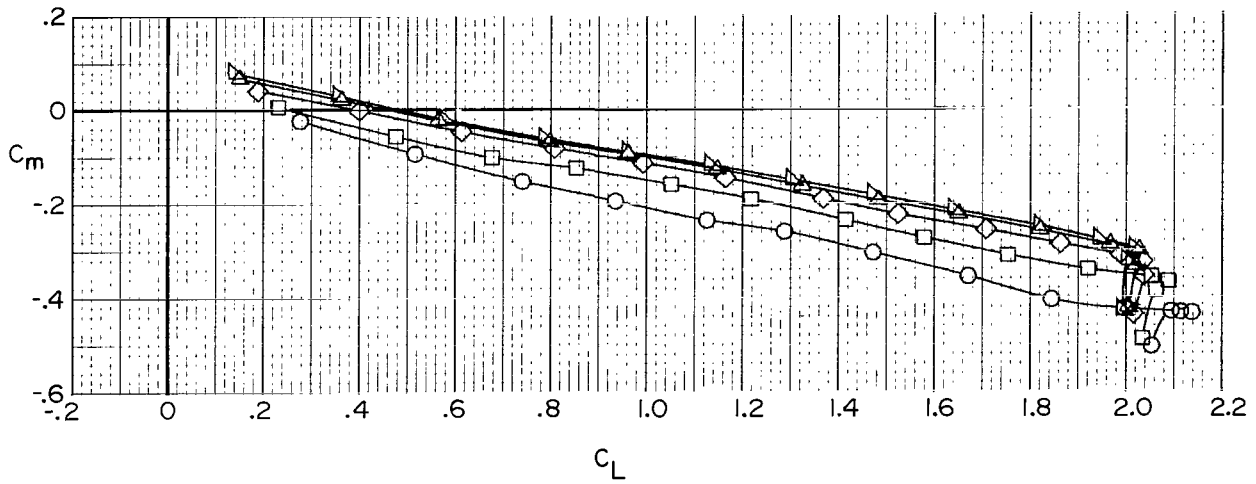

(b) Pitching-moment coefficient.

Figure 9.- Concluded.

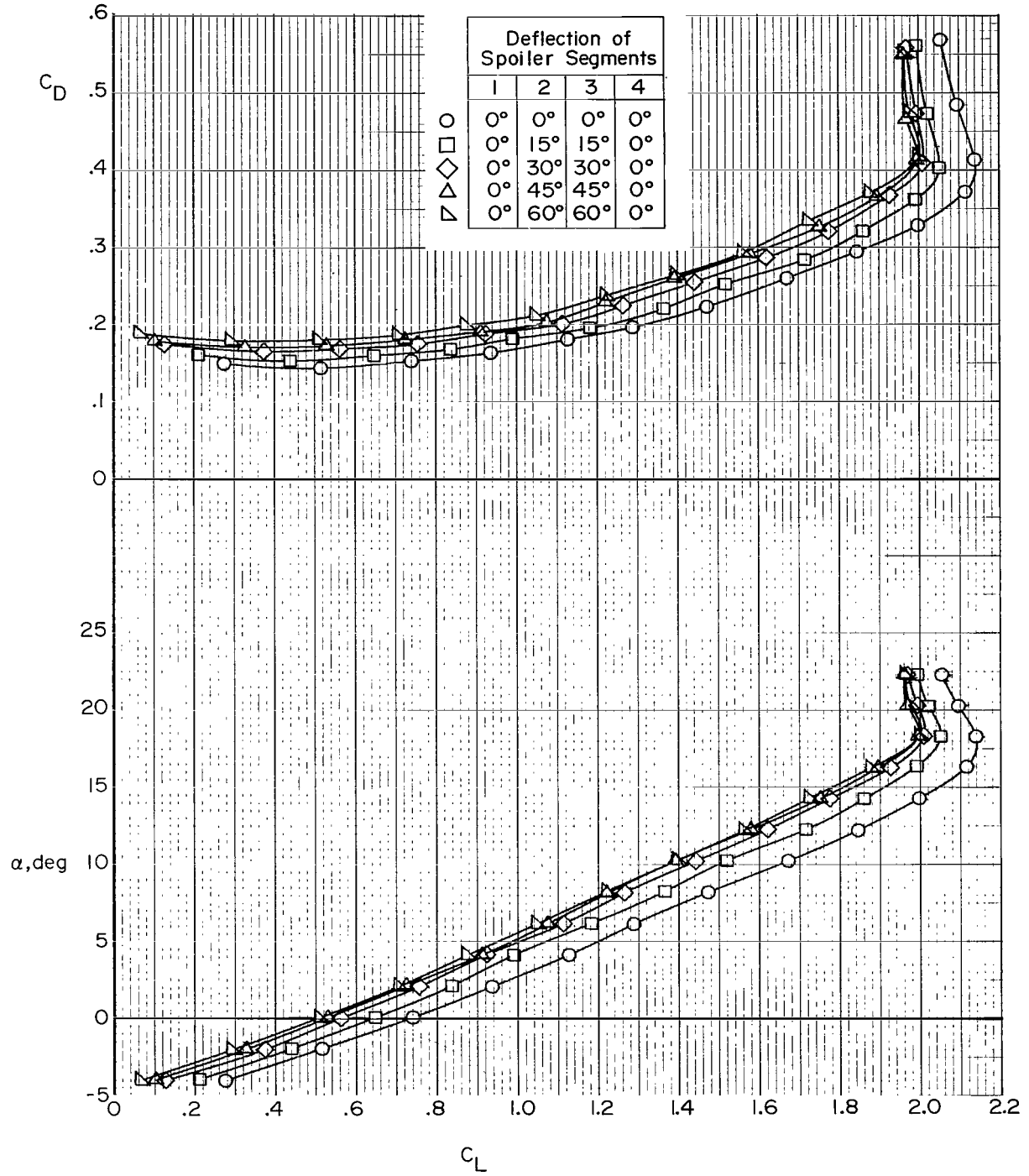

(a) Lift and drag coefficients.

Figure 10.- Effect of deflection angle of flight-spoiler segments 2 and 3 on longitudinal aerodynamic characteristics of transport aircraft model. $i_t = 0^o$; landing flap configuration.

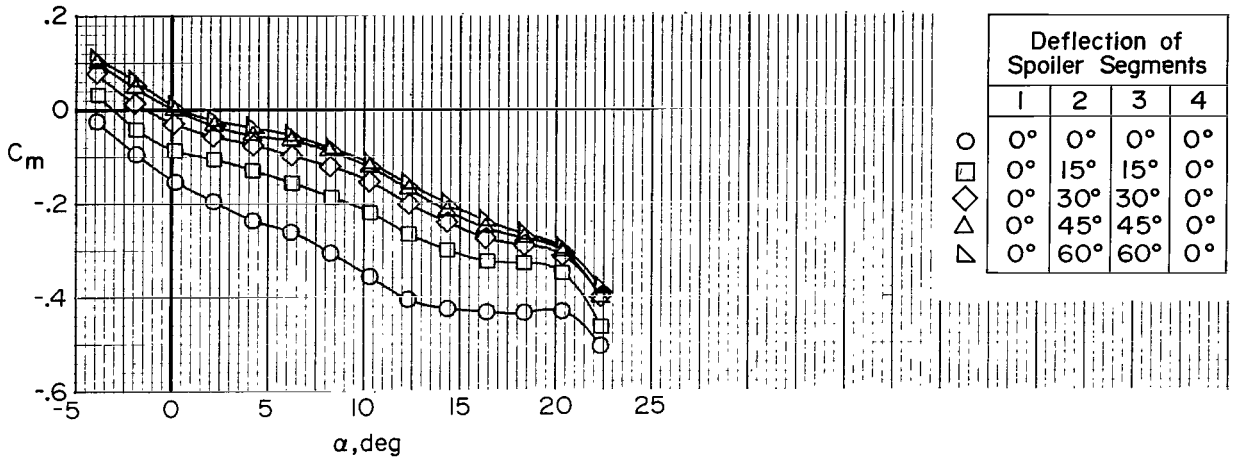

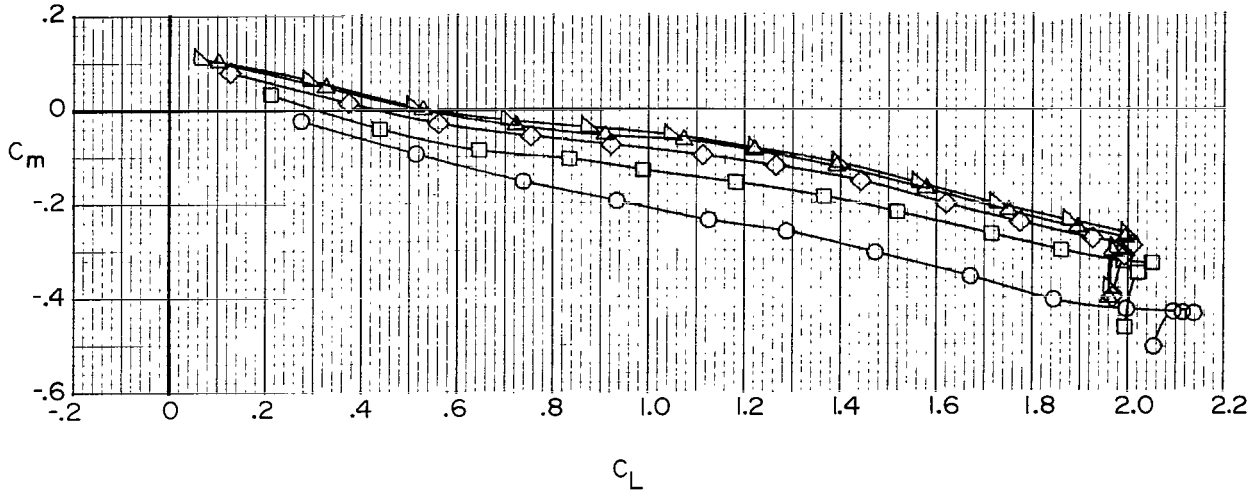

(b) Pitching-moment coefficient.

Figure 10.- Concluded.

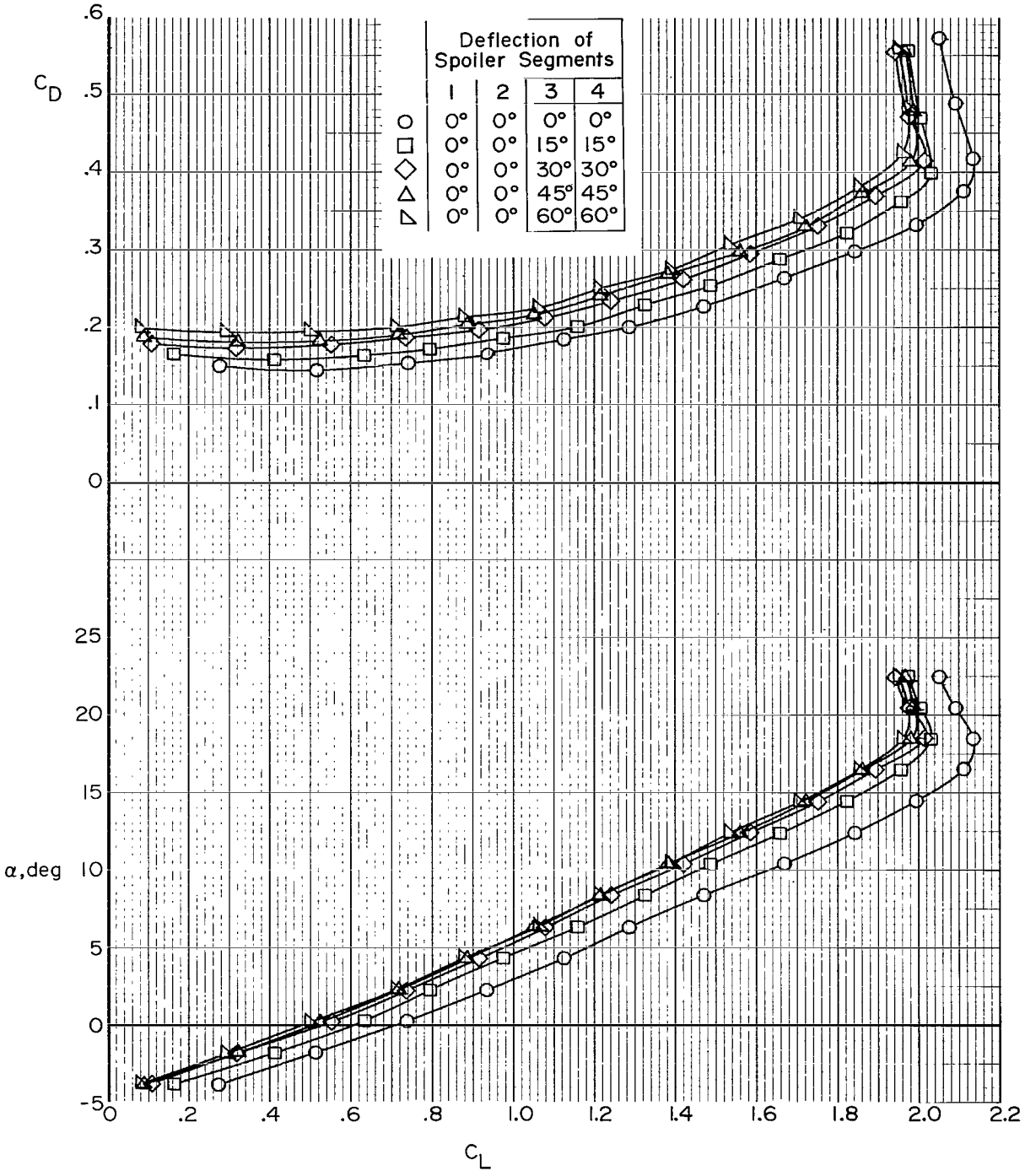

(a) Lift and drag coefficients.

Figure 11.- Effect of deflection angle of flight-spoiler segments 3 and 4 on longitudinal aerodynamic characteristics of transport aircraft model. $i_t = 0^o$; landing flap configuration.

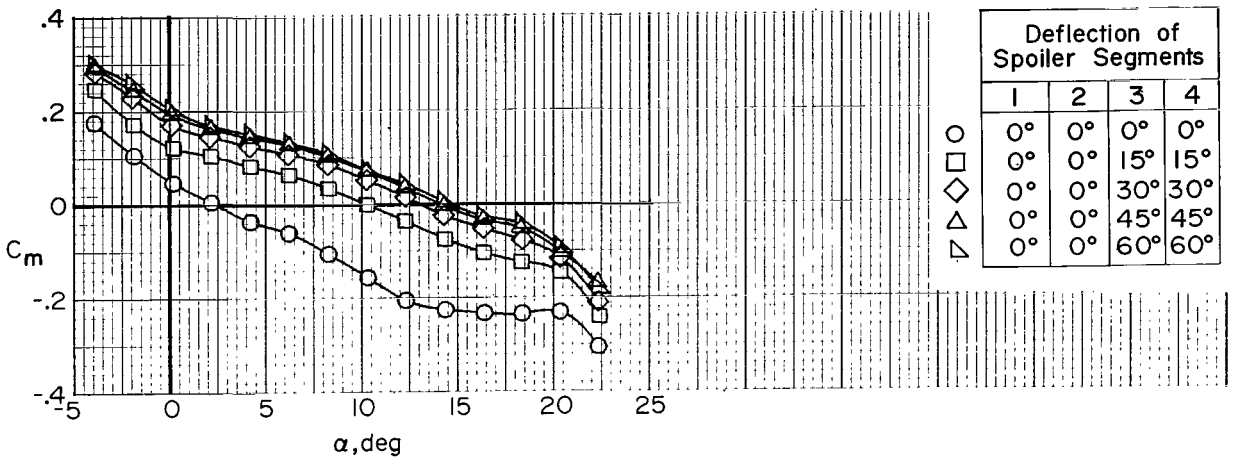

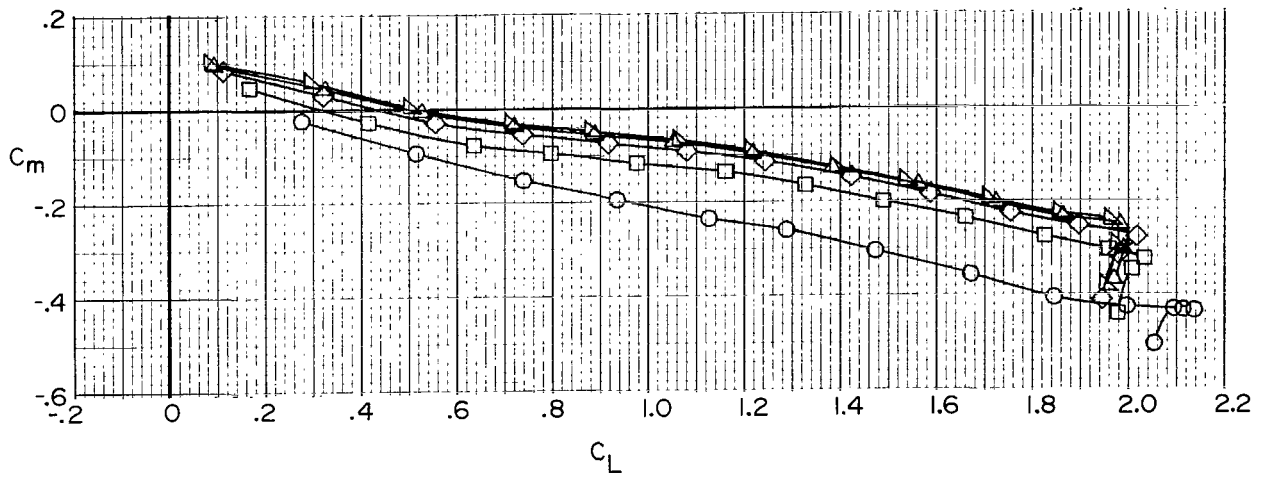

(b) Pitching-moment coefficient.

Figure 11.- Concluded.

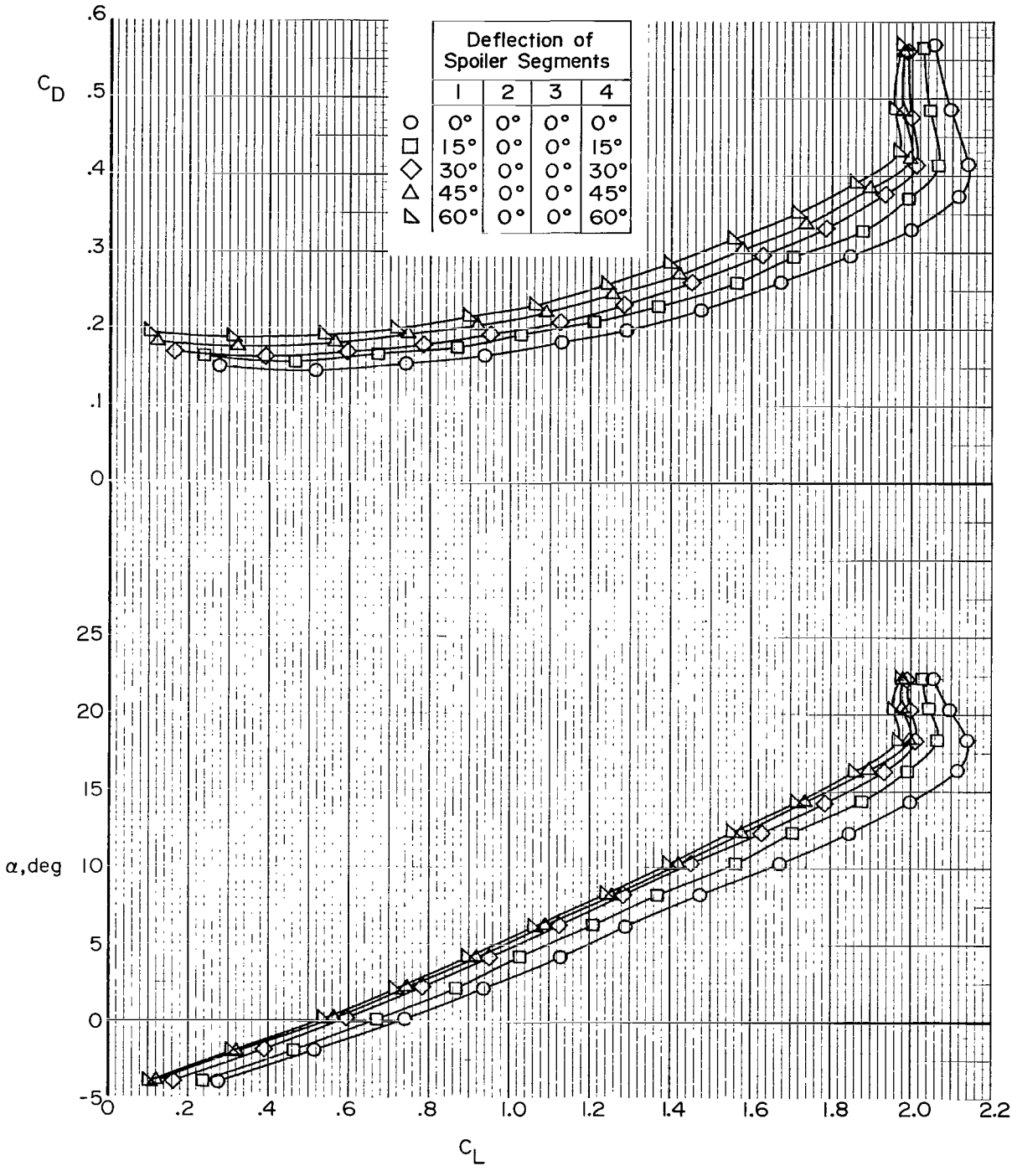

(a) Lift and drag coefficients.

Figure 12.- Effect of deflection angle of flight-spoiler segments 1 and 4 on longitudinal aerodynamic characteristics of transport aircraft model. $i_t = 0^o$; landing flap configuration.

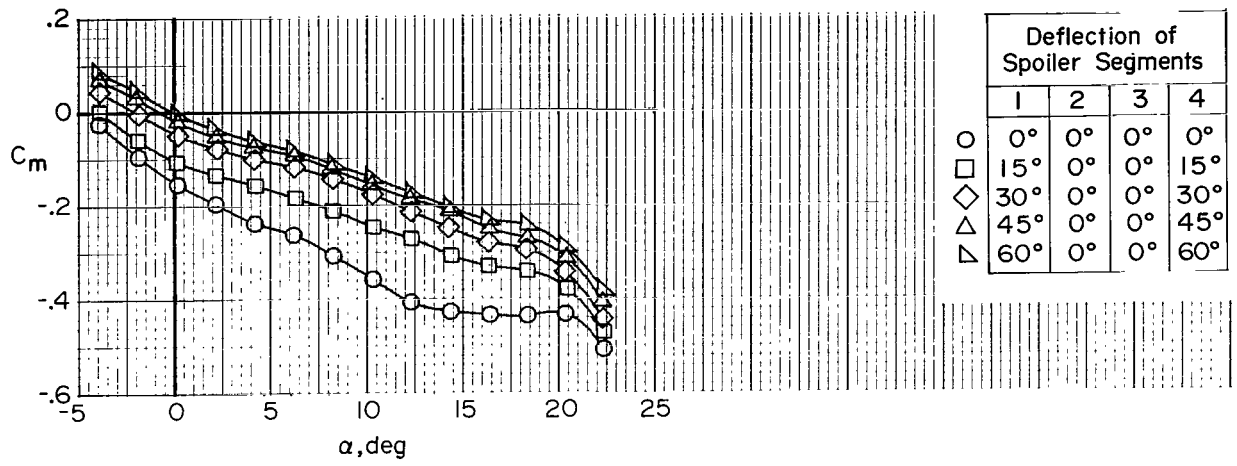

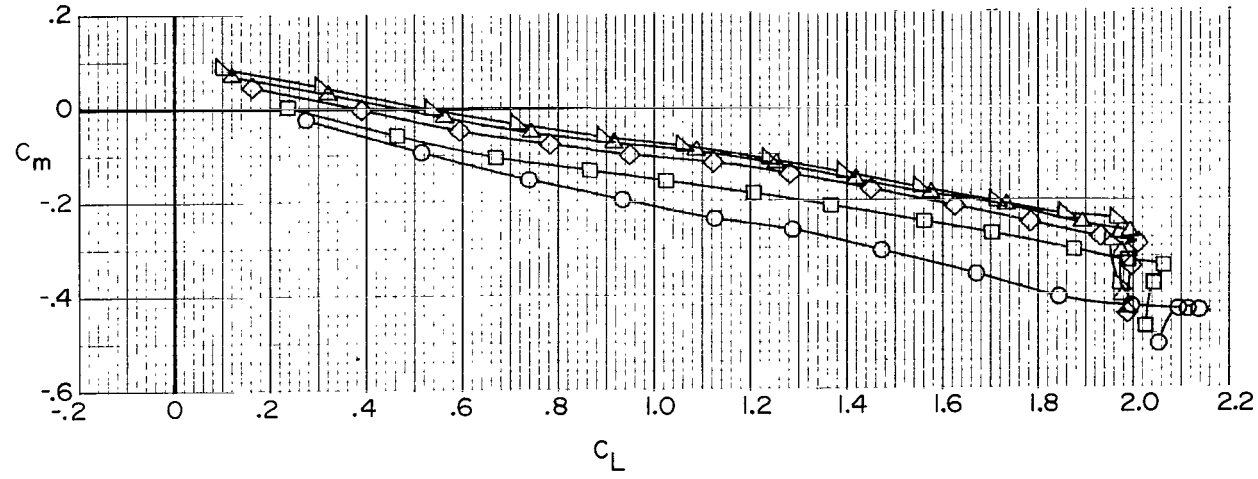

(b) Pitching-moment coefficient.

Figure 12.- Concluded.

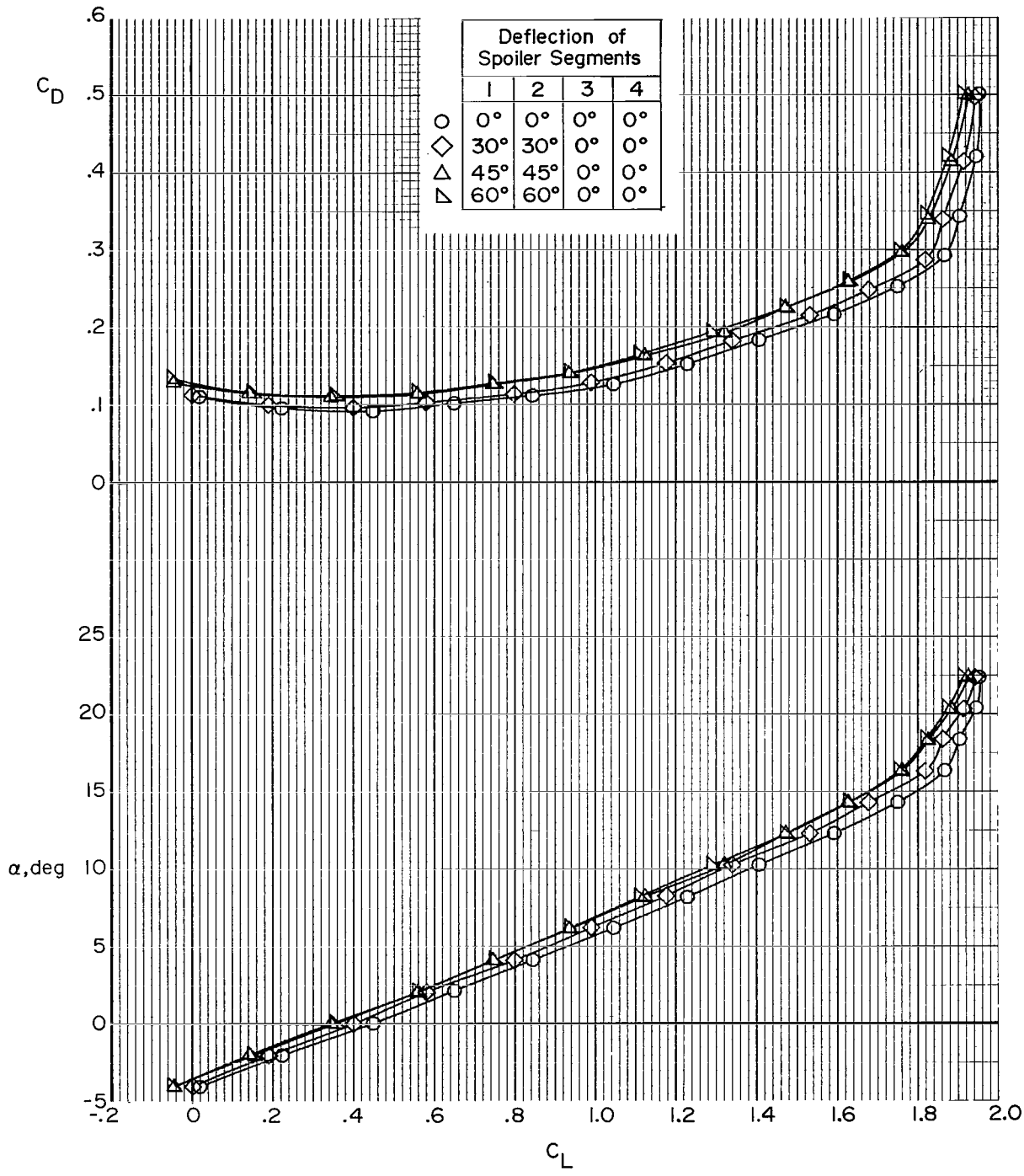

(a) Lift and drag coefficients.

Figure 13.- Effect of deflection angle of flight-spoiler segments 1 and 2 on longitudinal aerodynamic characteristics of transport aircraft model. $i_t = 0^o$; approach flap configuration.

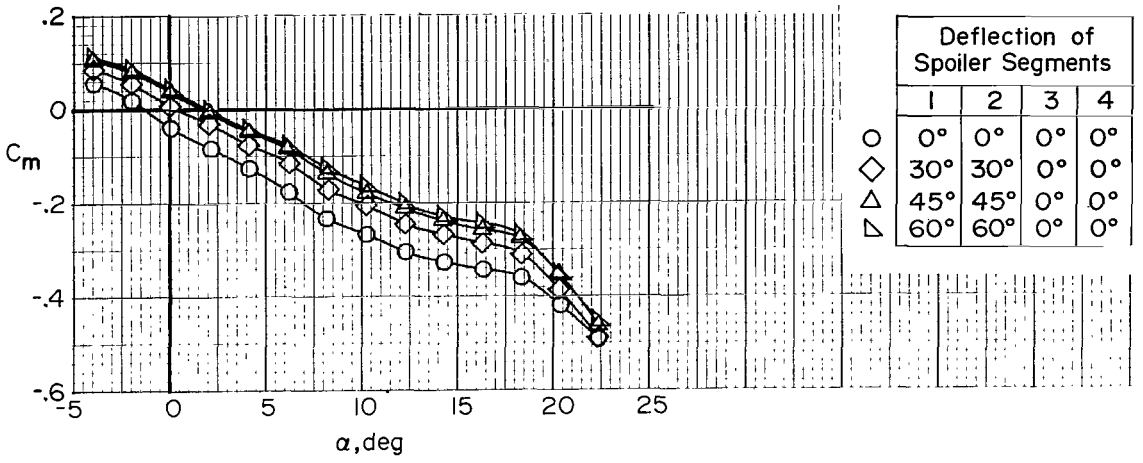

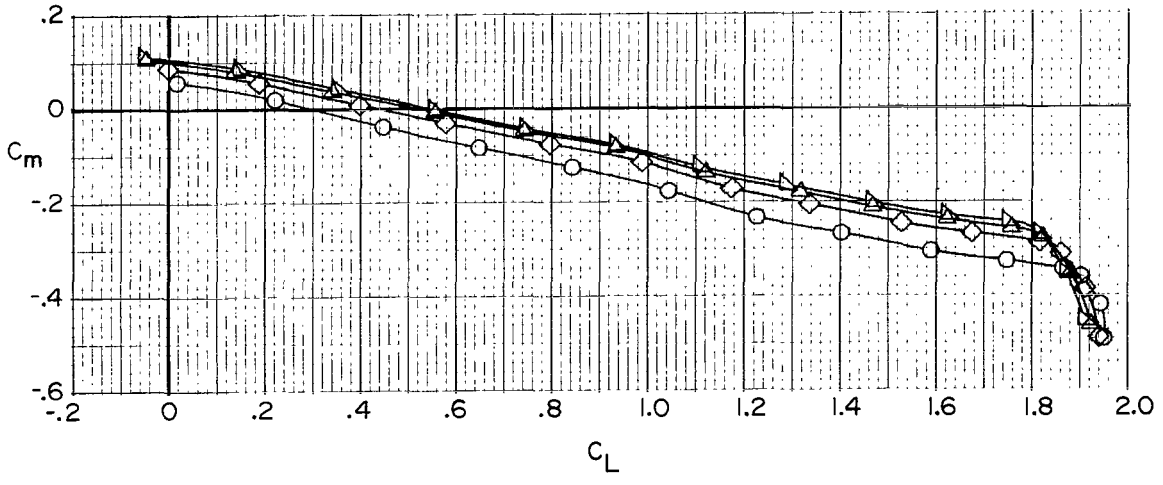

(b) Pitching-moment coefficient.

Figure 13.- Concluded.

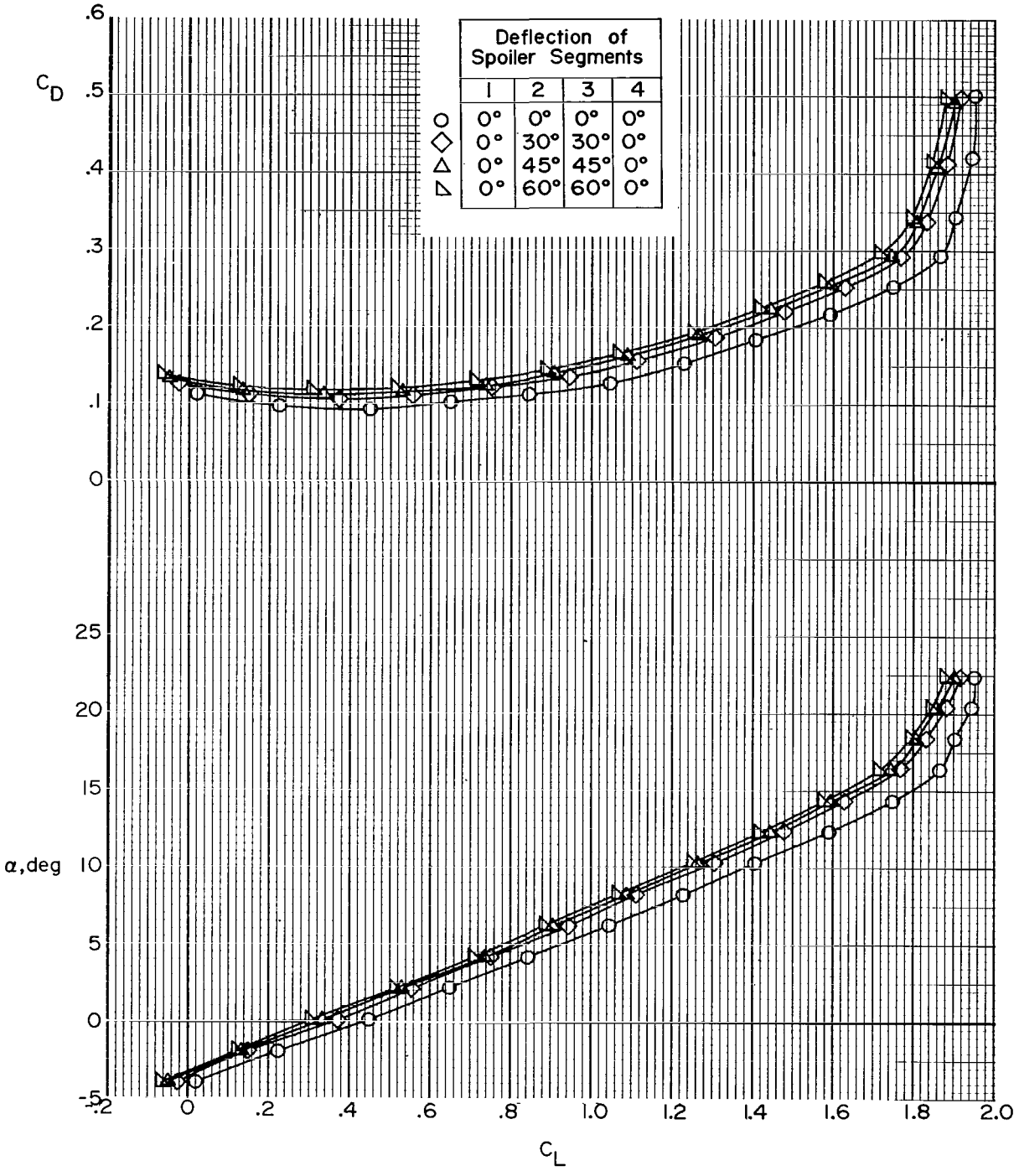

(a) Lift and drag coefficients.

Figure 14.- Effect of deflection angle of flight-spoiler segments 2 and 3 on longitudinal aerodynamic characteristics of transport aircraft model. $i_t = 0^o$; approach flap configuration.

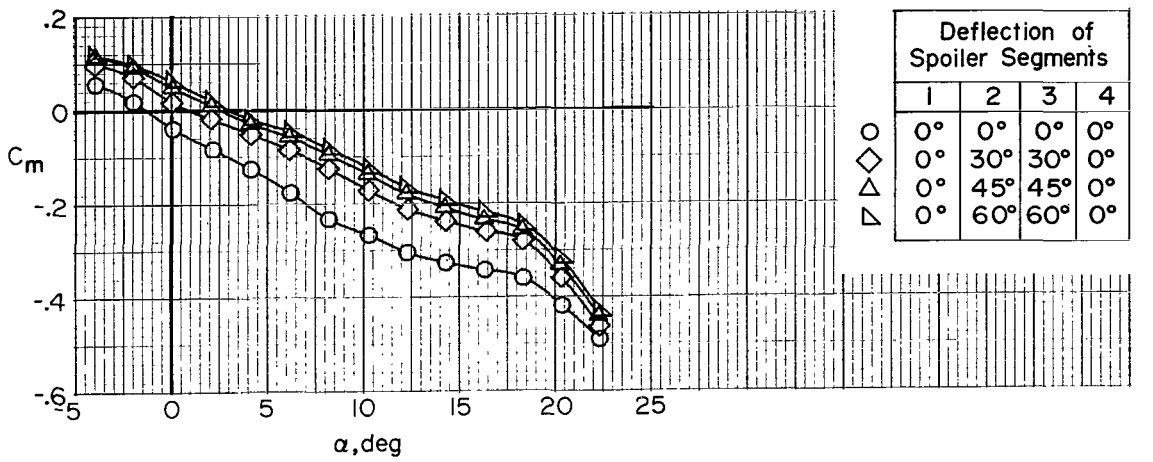

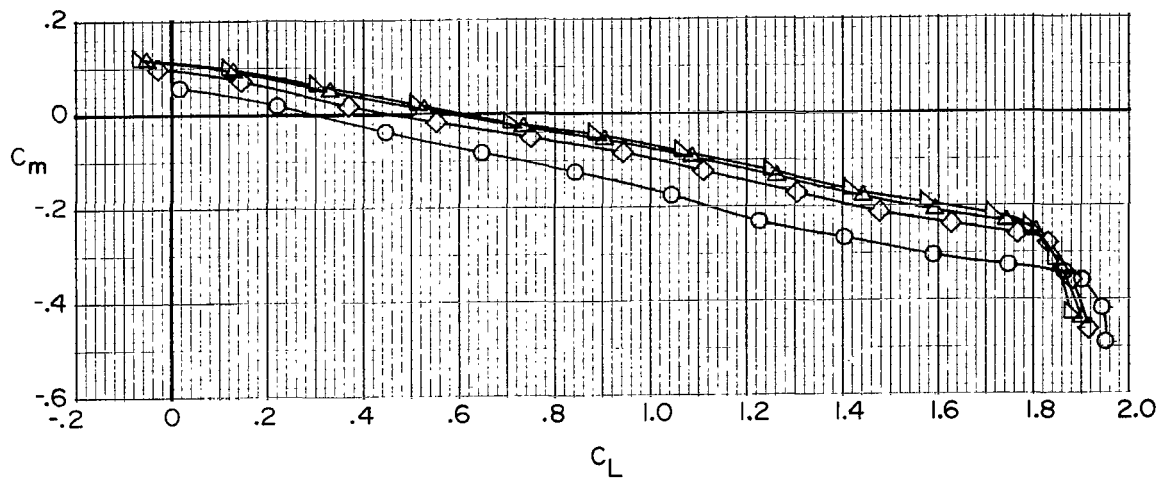

(b) Pitching-moment coefficient.

Figure 14.- Concluded.

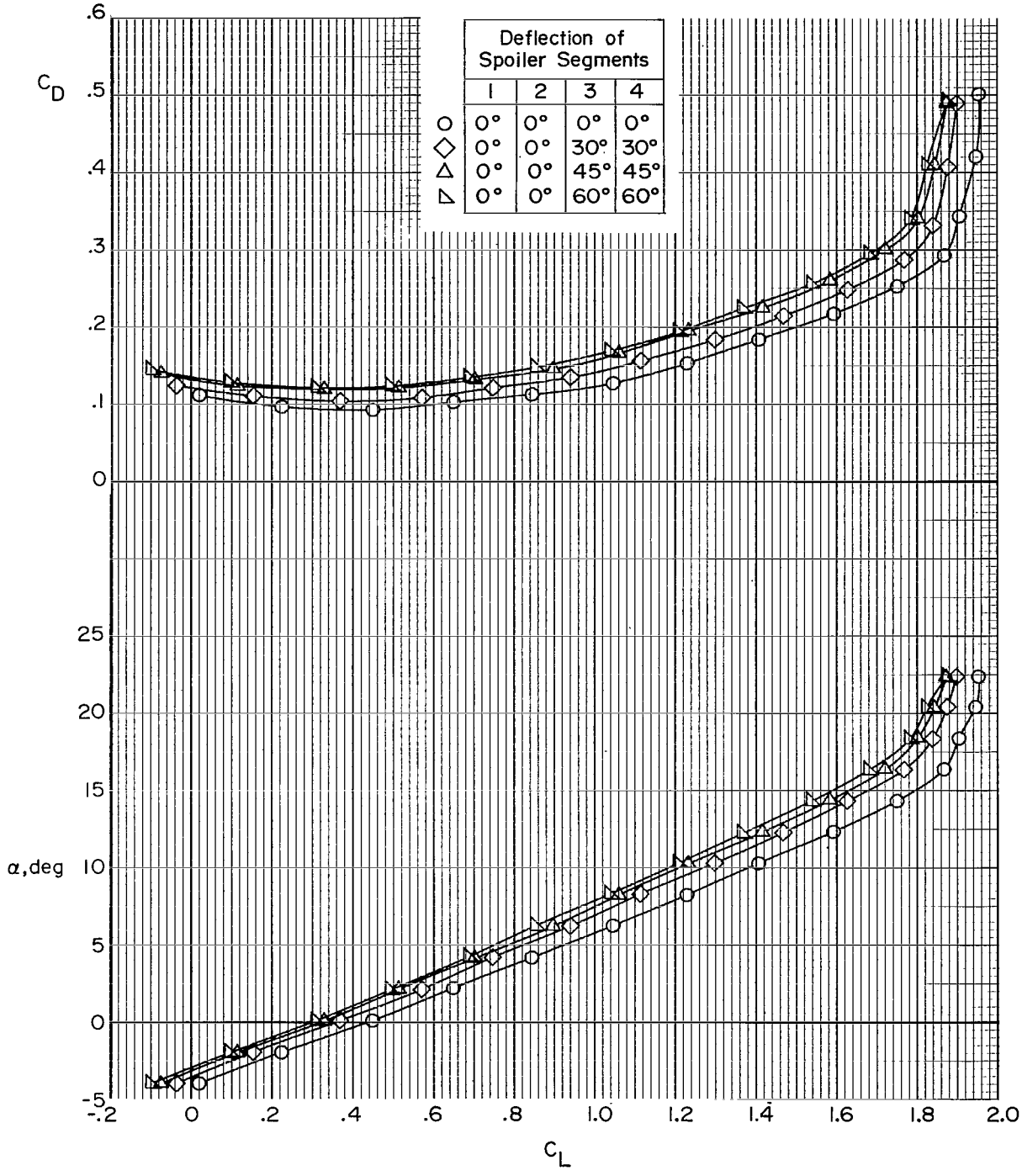

(a) Lift and drag coefficients.

Figure 15.- Effect of deflection angle of flight-spoiler segments 3 and 4 on longitudinal aerodynamic characteristics of transport aircraft model. $i_t = 0^o$; approach flap configuration.

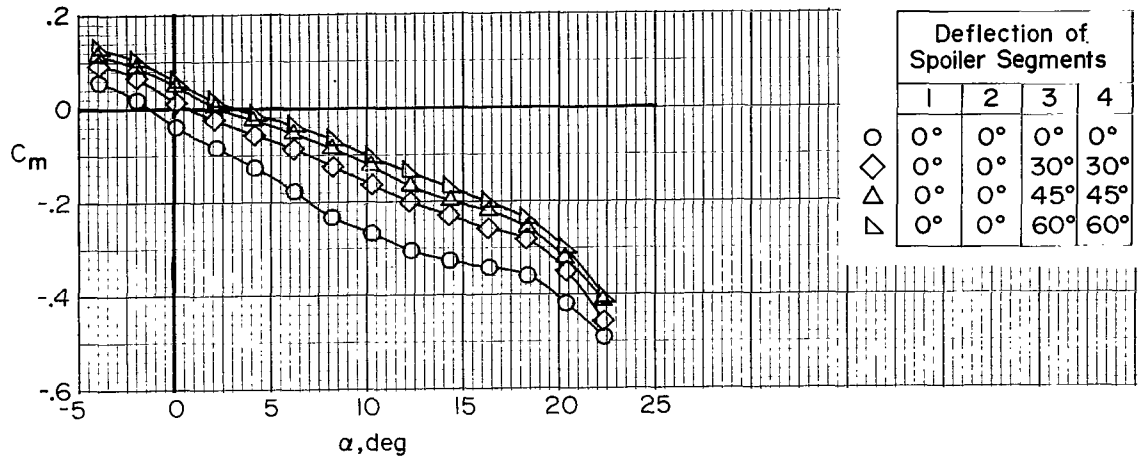

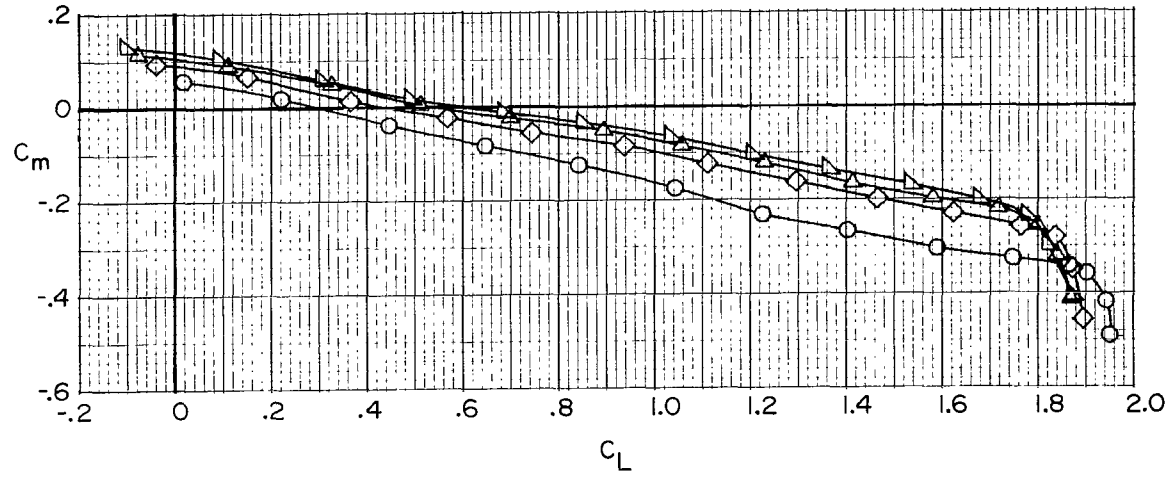

(b) Pitching-moment coefficient.

Figure 15.- Concluded.

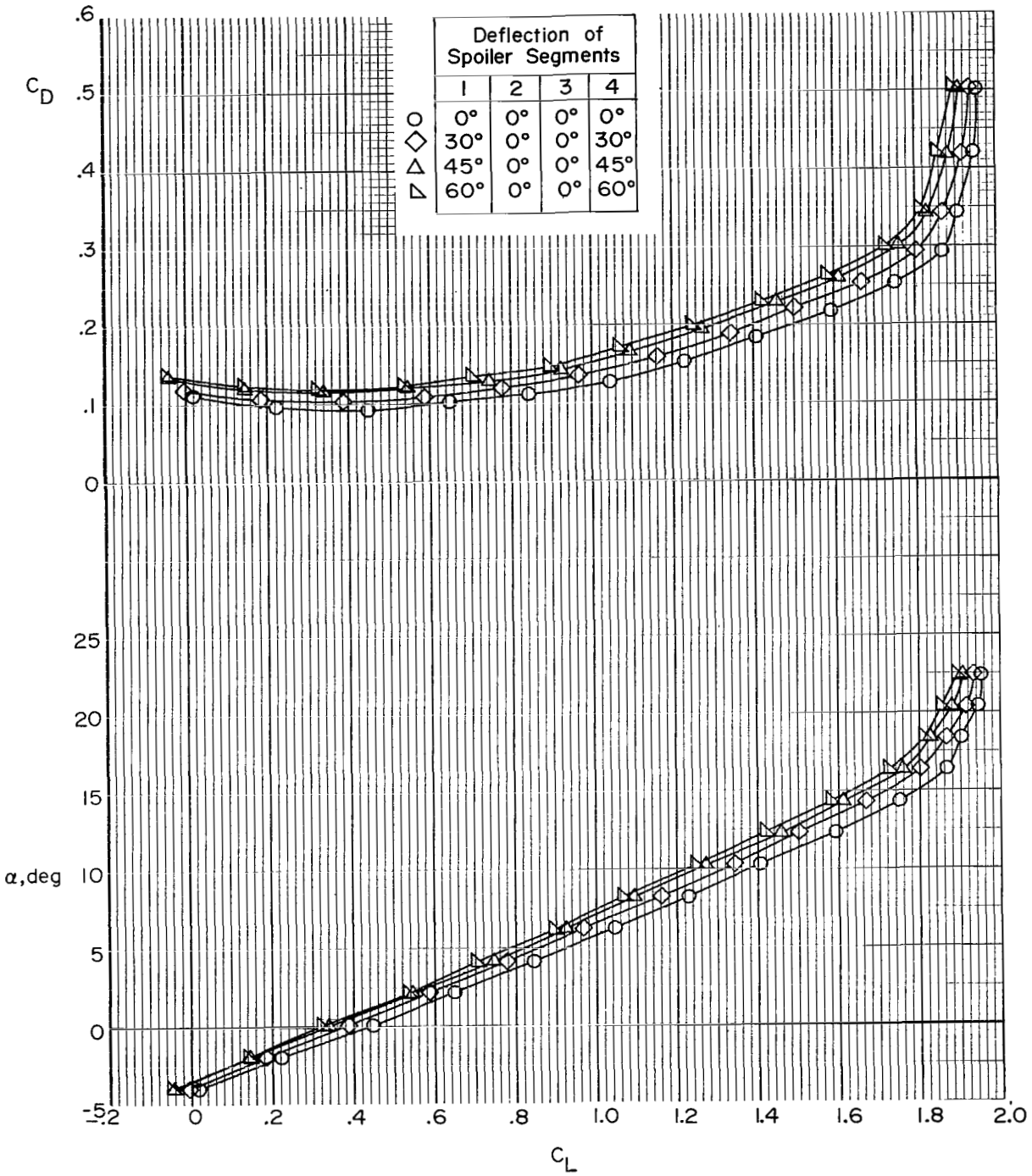

(a) Lift and drag coefficients.

Figure 16.- Effect of deflection angle of flight-spoiler segments 1 and 4 on longitudinal aerodynamic characteristics of transport aircraft model. $i_t = 0^o$; approach flap configuration.

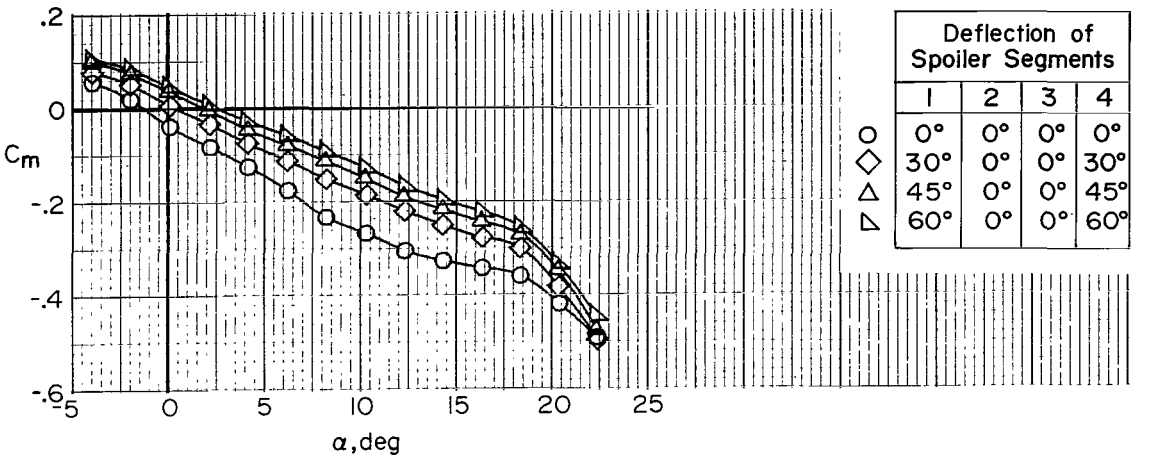

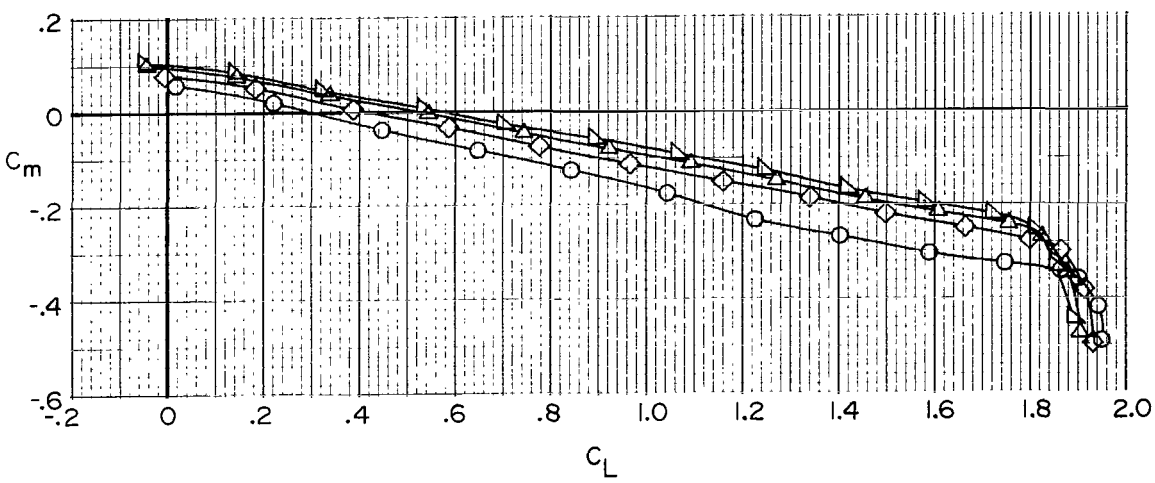

(b) Pitching-moment coefficient.

Figure 16.- Concluded.

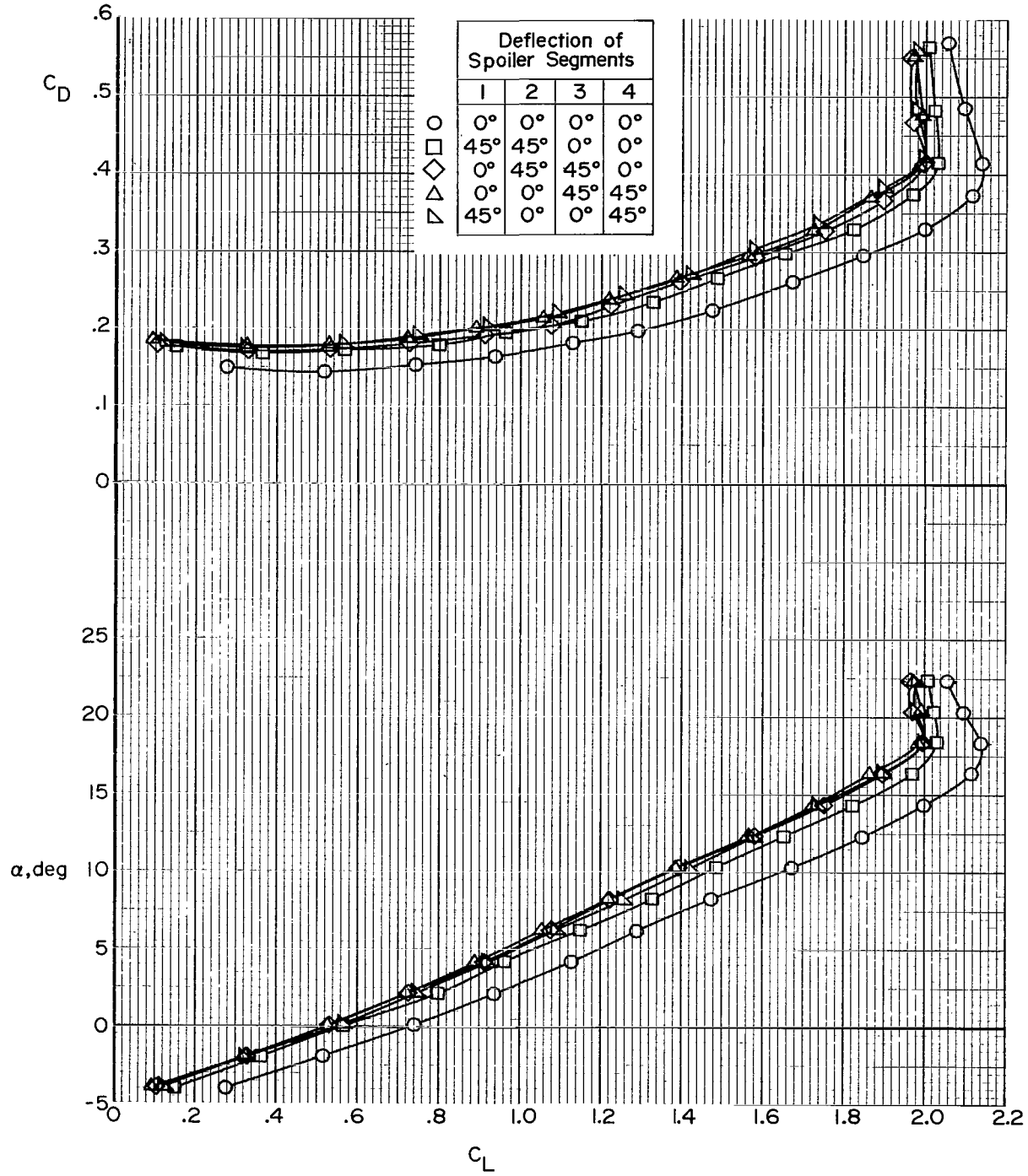

(a) Lift and drag coefficients.

Figure 17.- Effect of flight-spoiler segments 1 and 2, 2 and 3, 3 and 4, and 1 and 4 deflected 45° on longitudinal aerodynamic characteristics of transport aircraft model. $i_t = 0°$; landing flap configuration.

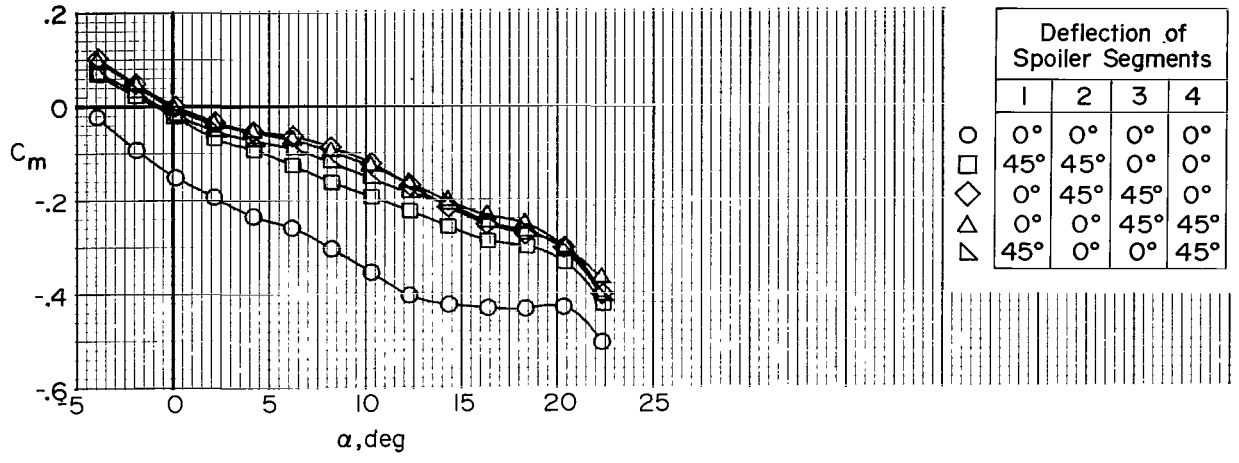

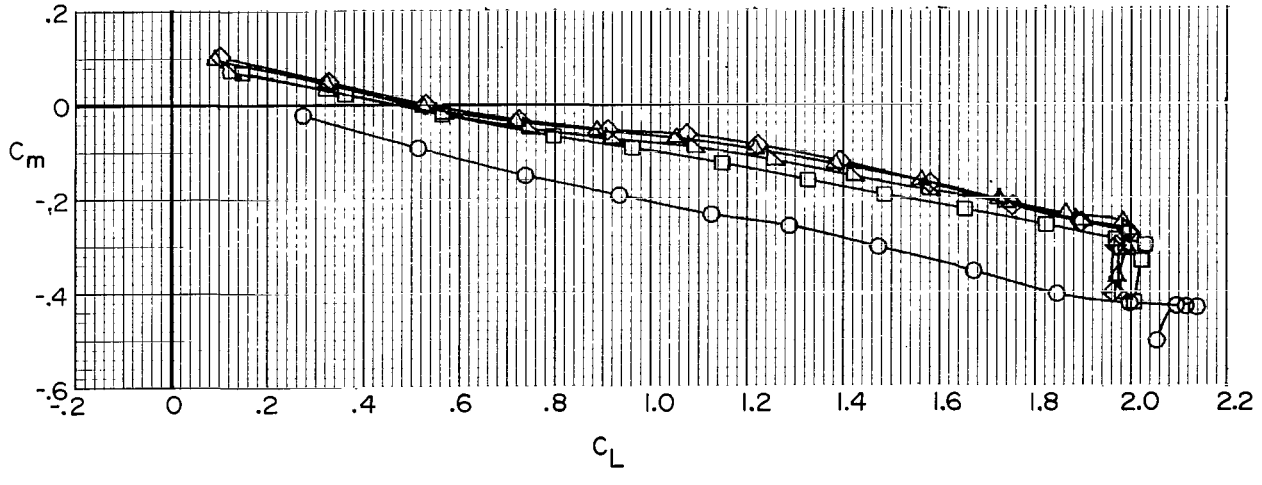

(b) Pitching-moment coefficient.

Figure 17.- Concluded.

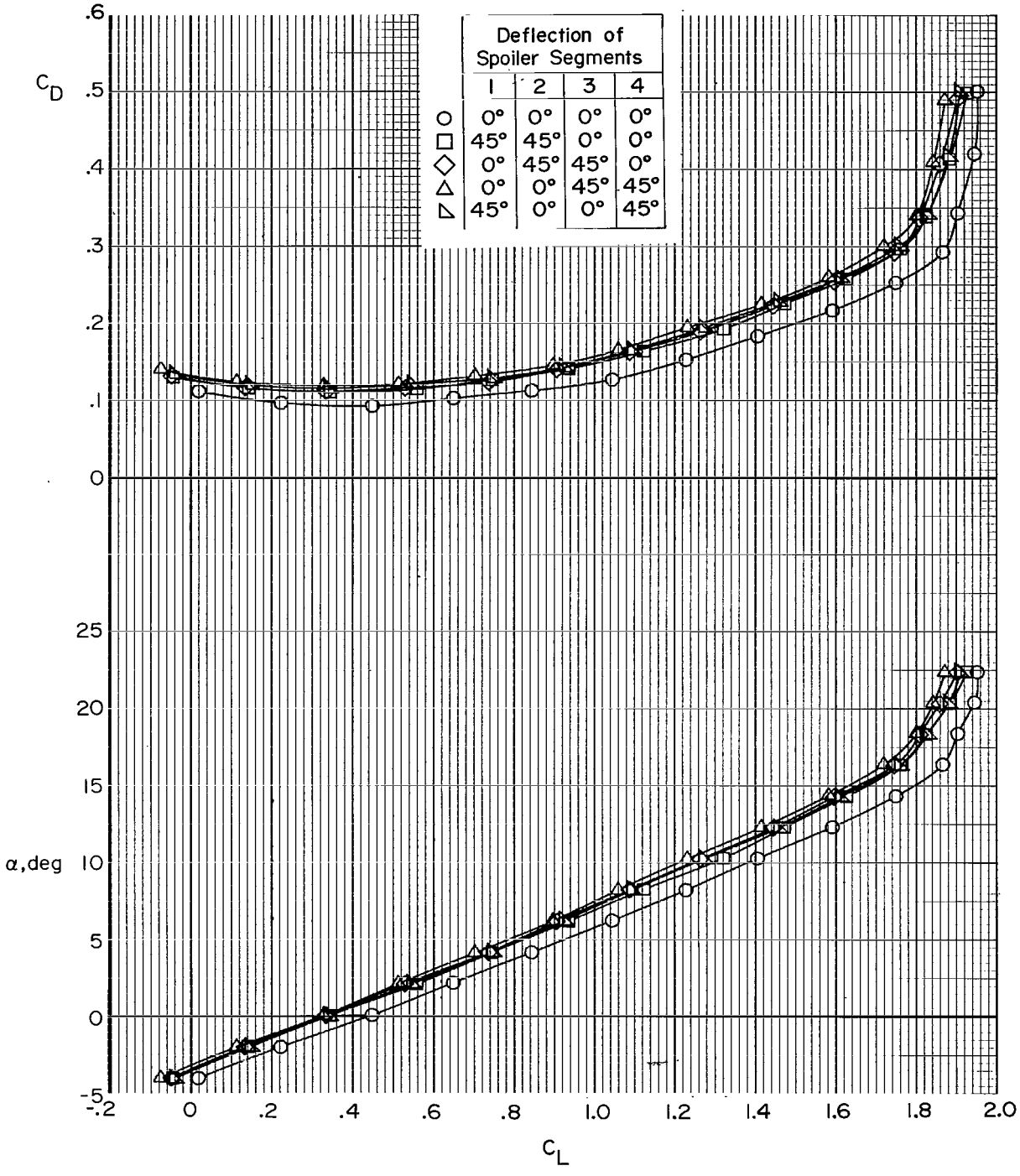

(a) Lift and drag coefficients.

Figure 18.- Effect of flight-spoiler segments 1 and 2, 2 and 3, 3 and 4, and 1 and 4 deflected 45° on longitudinal aerodynamic characteristics of transport aircraft model. i_t = 0°; approach flap configuration.

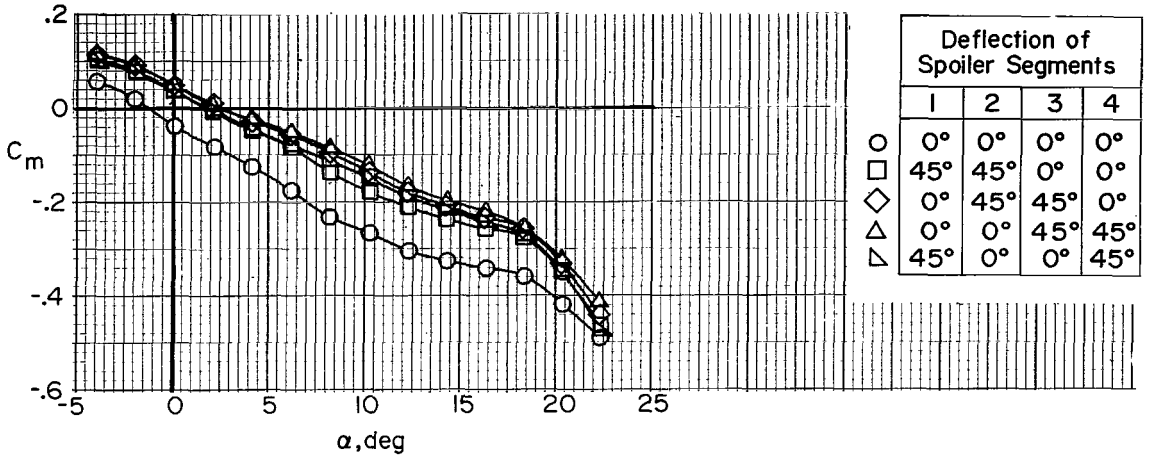

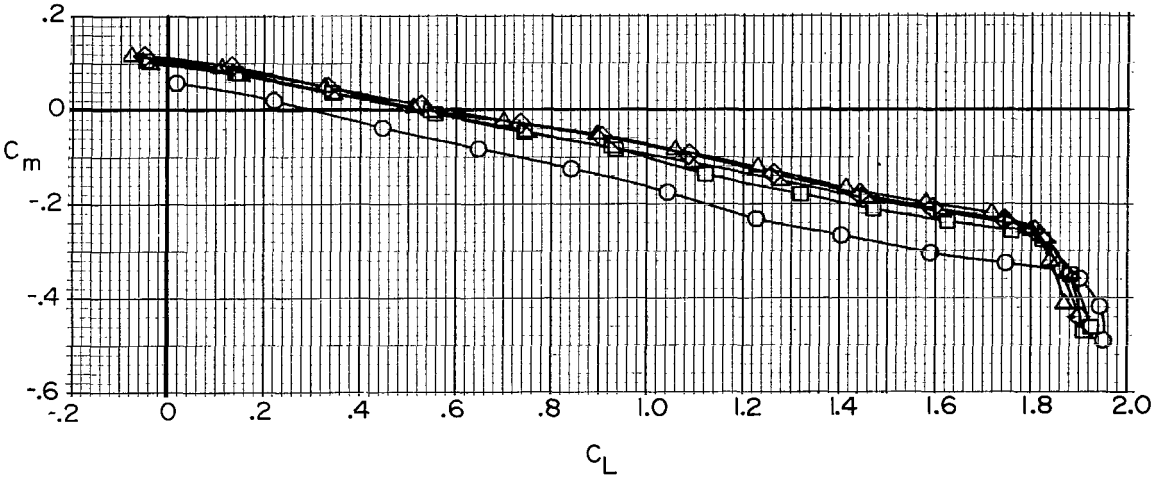

(b) Pitching-moment coefficient.

Figure 18.- Concluded.

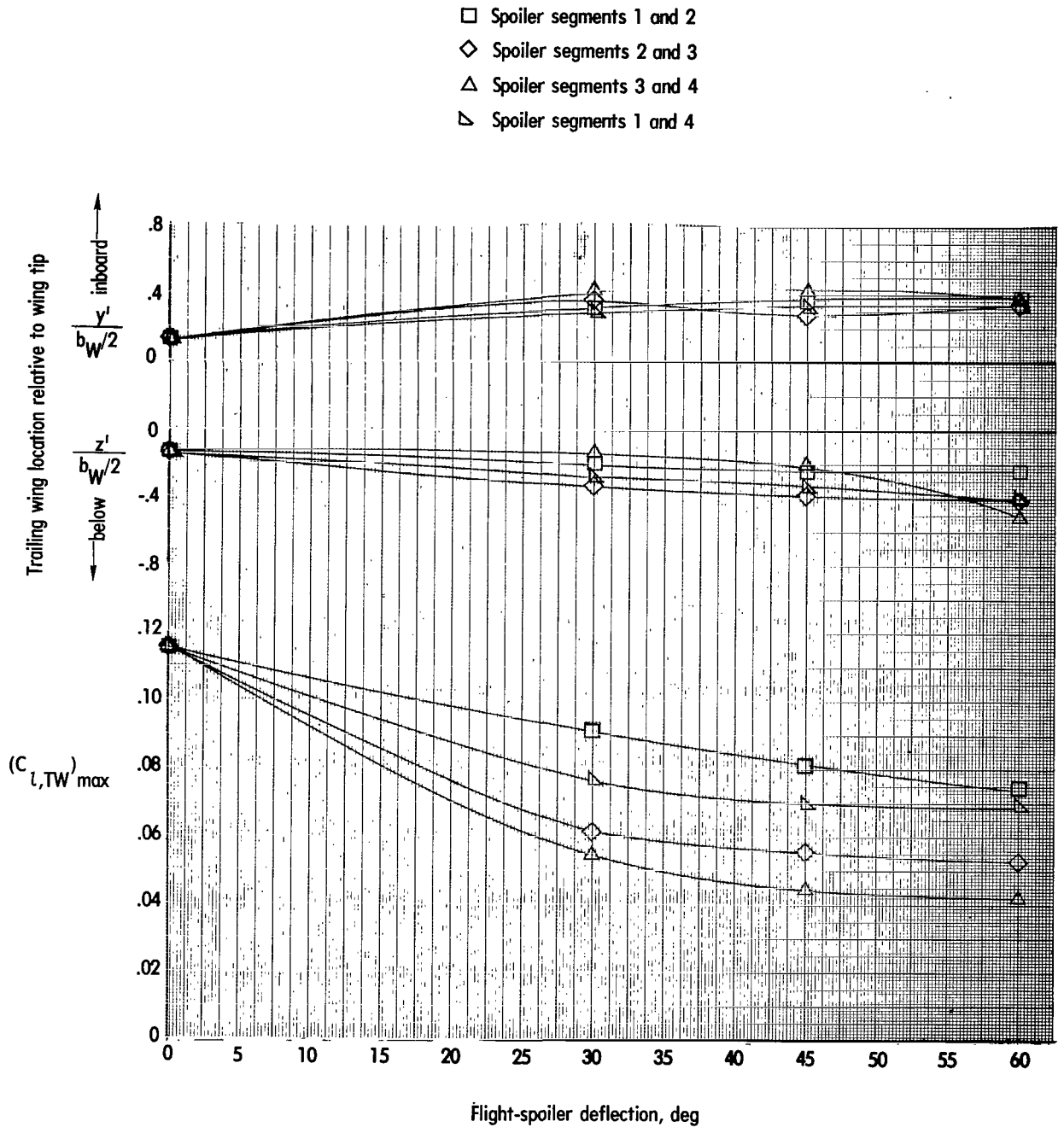

Figure 19.- Variation of trailing wing location and rolling-moment coefficient with flight-spoiler deflection for various segments of flight spoilers. Trailing wing model located 9.8 transport wing spans behind transport aircraft model; $C_{L,trim}$ = 1.2; approach flap configuration.

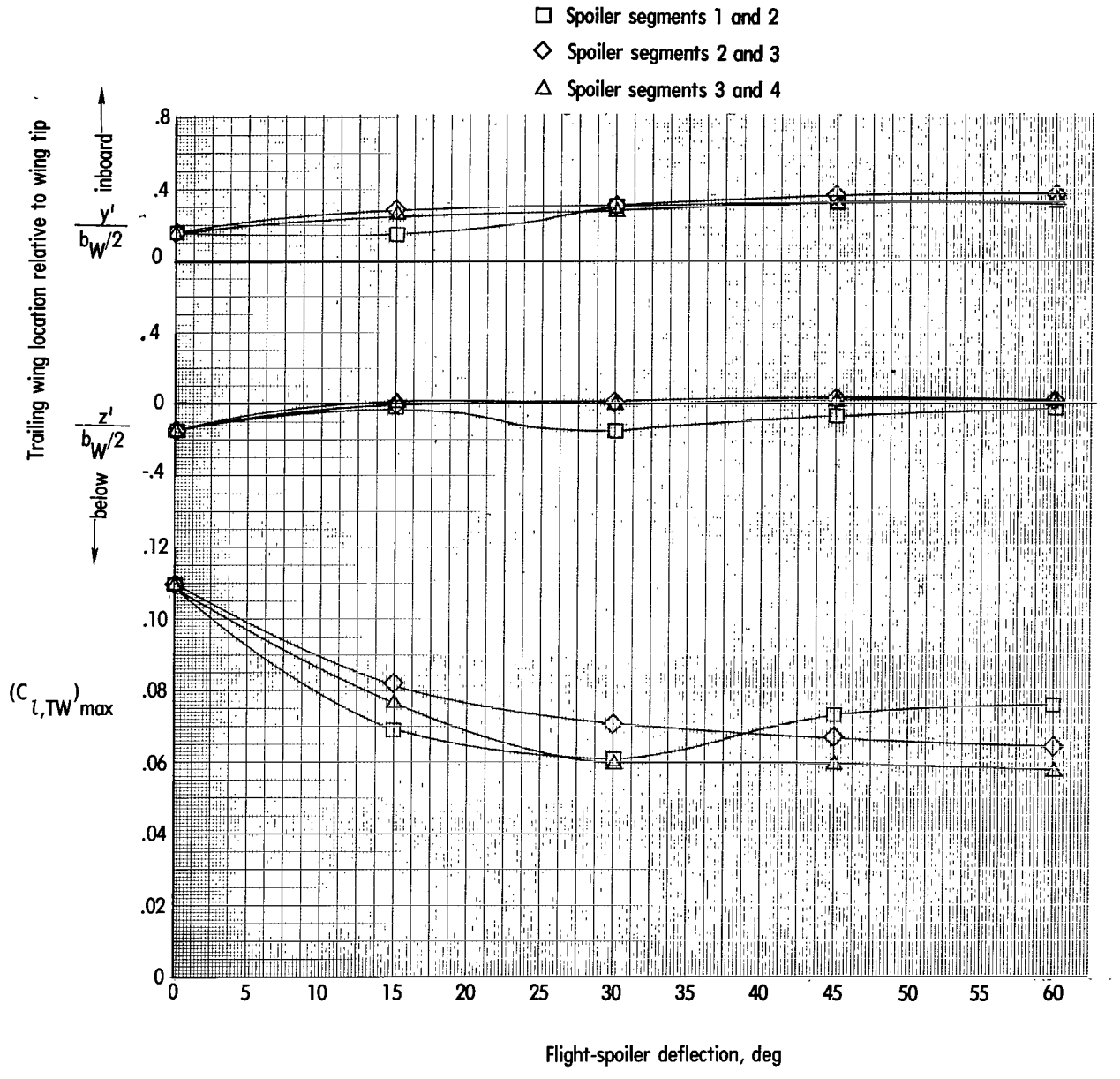

Figure 20.- Variation of trailing wing location and rolling-moment coefficient with flight-spoiler deflection for various segments of flight spoilers. Trailing wing model located 3.9 transport wing spans behind transport aircraft model; $C_{L,trim}$ = 1.2; landing flap configuration.

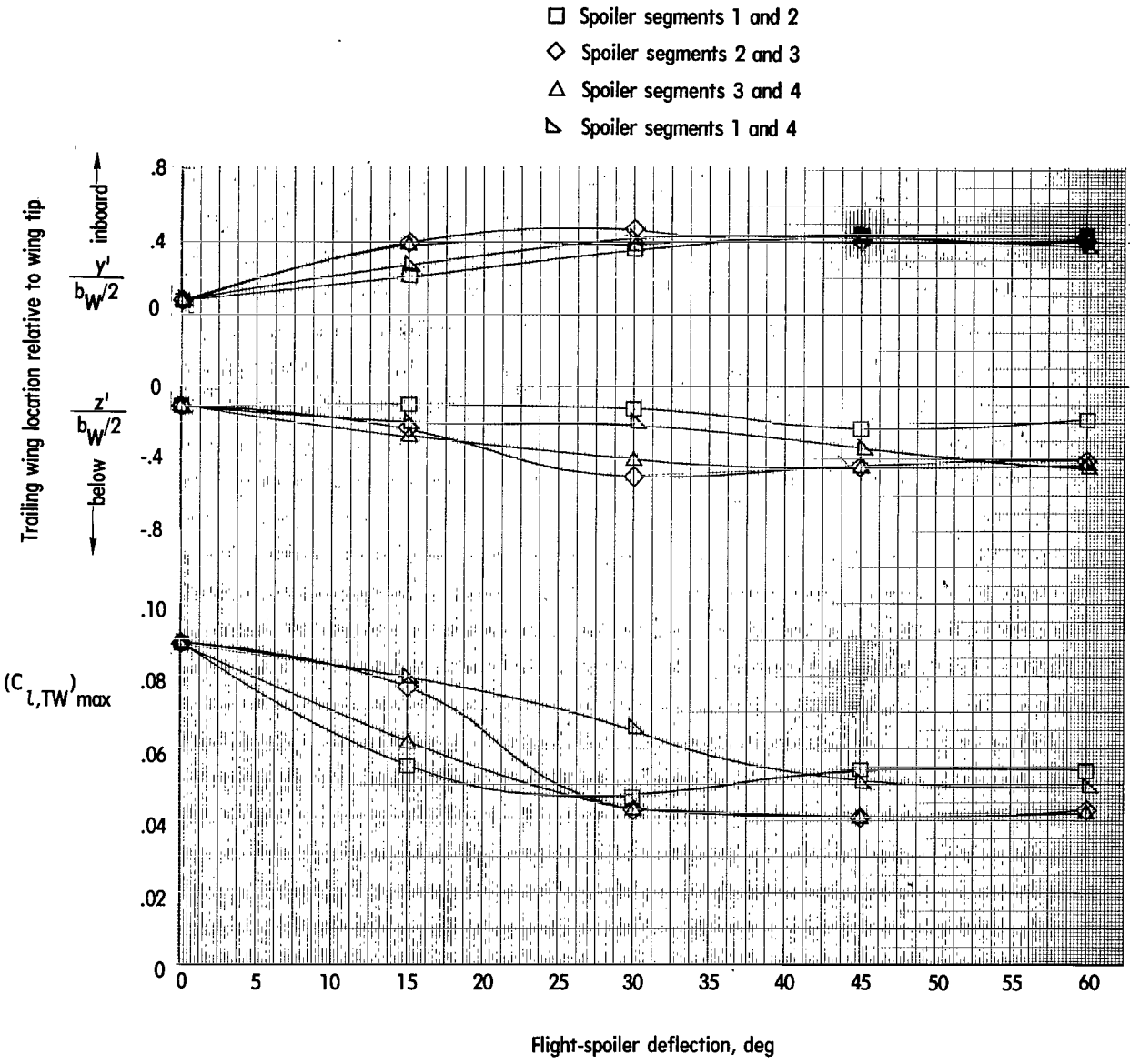

Figure 21.- Variation of trailing wing location and rolling-moment coefficient with flight-spoiler deflection for various segments of flight spoilers. Trailing wing model located 9.8 transport wing spans behind transport aircraft model; $C_{L,trim}$ = 1.2; landing flap configuration.

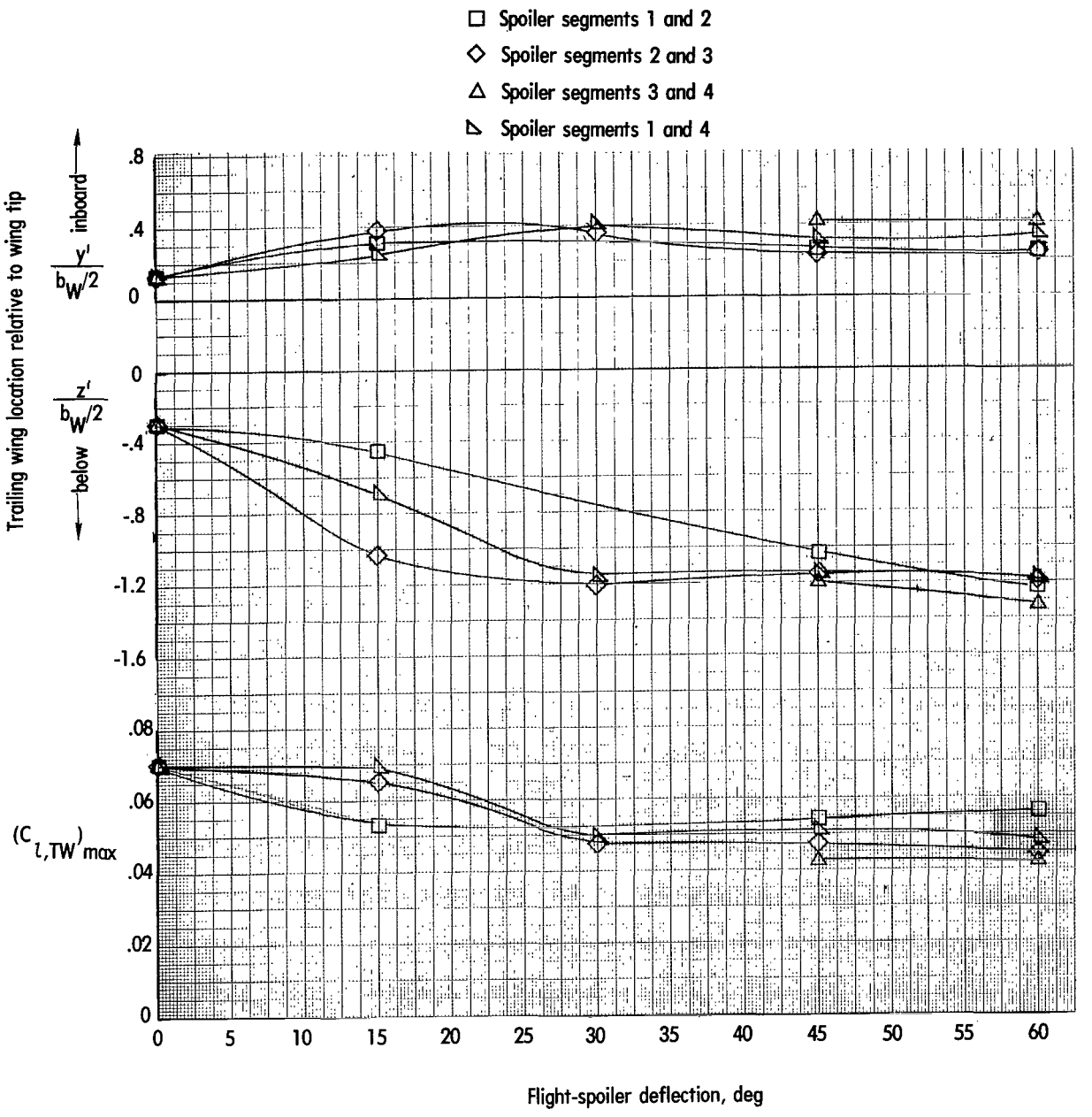

Figure 22.- Variation of trailing wing location and rolling-moment coefficient with flight-spoiler deflection for various segments of flight spoilers. Trailing wing model located 19.6 transport wing spans behind transport aircraft model; $C_{L,trim}$ = 1.2; landing flap configuration.

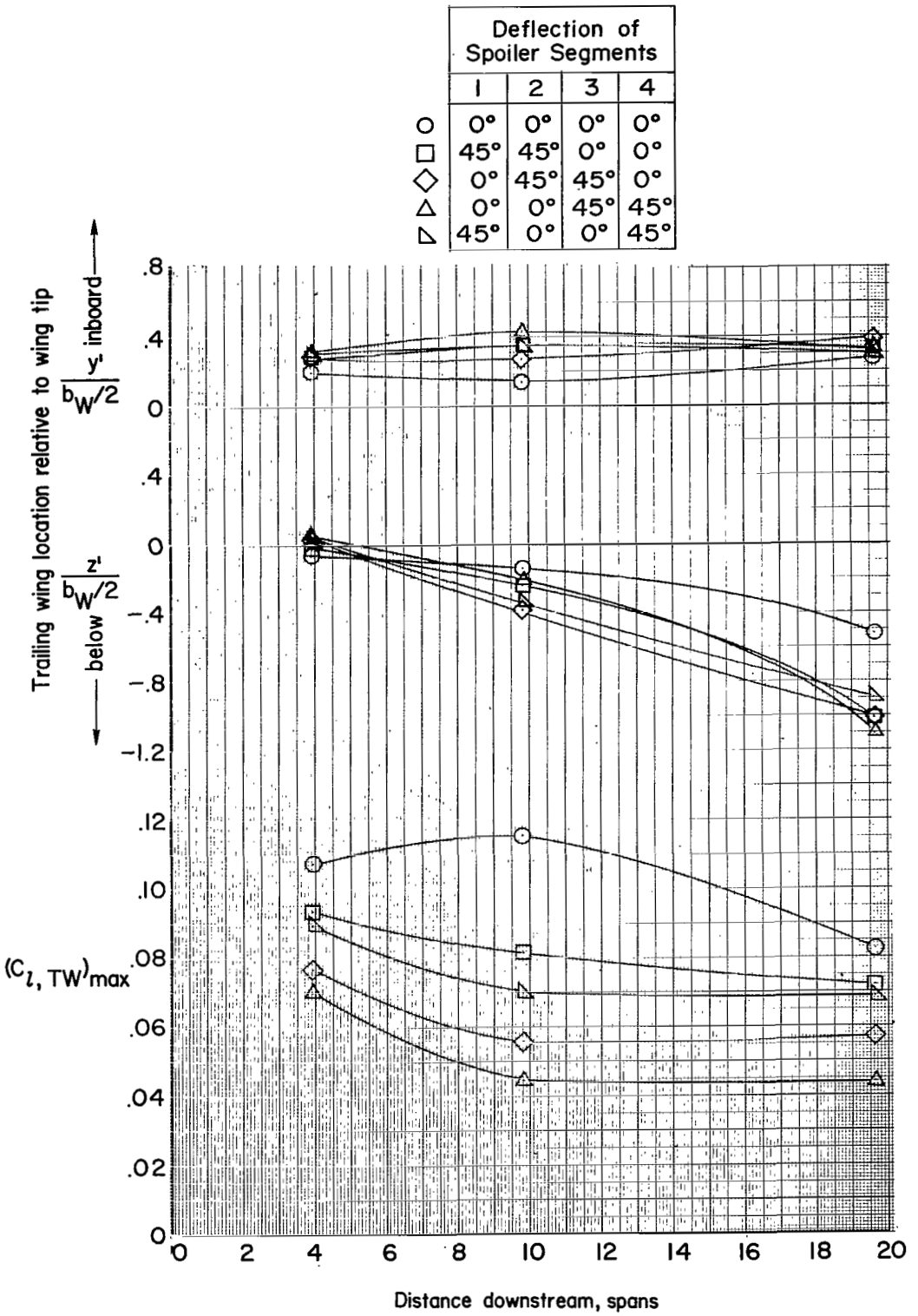

Figure 23.- Variation of trailing wing location and rolling-moment coefficient with downstream distance behind transport aircraft model (distance given in transport wing spans) with various segments of flight spoilers deflected 45°. $C_{L,trim}$ = 1.2; approach flap configuration.

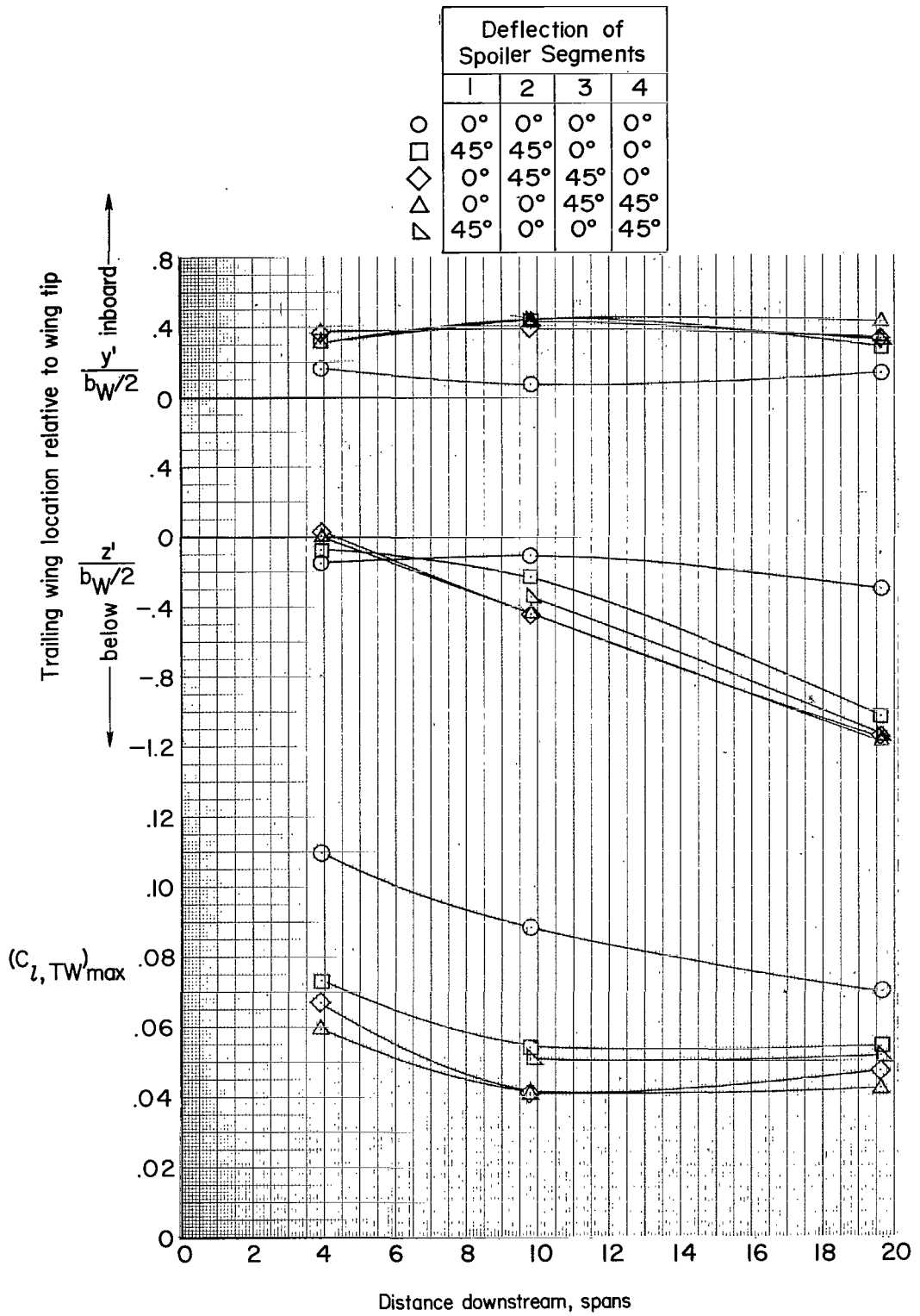

Figure 24.- Variation of trailing wing location and rolling-moment coefficient with downstream distance behind transport aircraft model (distance given in transport wing spans) with various segments of flight spoilers deflected 45°. $C_{L,trim} = 1.2$; landing flap configuration.

NATIONAL AERONAUTICS AND SPACE ADMINISTRATION
WASHINGTON, D.C. 20546

OFFICIAL BUSINESS
PENALTY FOR PRIVATE USE $300

SPECIAL FOURTH-CLASS RATE BOOK

POSTAGE AND FEES PAID
NATIONAL AERONAUTICS AND SPACE ADMINISTRATION
451

U.S.MAIL

916 001 C1 U A 761112 S00903DS
DEPT OF THE AIR FORCE
AF WEAPONS LABORATORY
ATTN: TECHNICAL LIBRARY (SUL)
KIRTLAND AFB NM 87117

POSTMASTER: If Undeliverable (Section 158 Postal Manual) Do Not Return

"The aeronautical and space activities of the United States shall be conducted so as to contribute . . . to the expansion of human knowledge of phenomena in the atmosphere and space. The Administration shall provide for the widest practicable and appropriate dissemination of information concerning its activities and the results thereof."

—NATIONAL AERONAUTICS AND SPACE ACT OF 1958

NASA SCIENTIFIC AND TECHNICAL PUBLICATIONS

TECHNICAL REPORTS: Scientific and technical information considered important, complete, and a lasting contribution to existing knowledge.

TECHNICAL NOTES: Information less broad in scope but nevertheless of importance as a contribution to existing knowledge.

TECHNICAL MEMORANDUMS: Information receiving limited distribution because of preliminary data, security classification, or other reasons. Also includes conference proceedings with either limited or unlimited distribution.

CONTRACTOR REPORTS: Scientific and technical information generated under a NASA contract or grant and considered an important contribution to existing knowledge.

TECHNICAL TRANSLATIONS: Information published in a foreign language considered to merit NASA distribution in English.

SPECIAL PUBLICATIONS: Information derived from or of value to NASA activities. Publications include final reports of major projects, monographs, data compilations, handbooks, sourcebooks, and special bibliographies.

TECHNOLOGY UTILIZATION PUBLICATIONS: Information on technology used by NASA that may be of particular interest in commercial and other non-aerospace applications. Publications include Tech Briefs, Technology Utilization Reports and Technology Surveys.

Details on the availability of these publications may be obtained from:

SCIENTIFIC AND TECHNICAL INFORMATION OFFICE

NATIONAL AERONAUTICS AND SPACE ADMINISTRATION

Washington, D.C. 20546